ESAIM: M2AN 60 (2026) 1635–1665
https://doi.org/10.1051/m2an/2026043

ESAIM: Mathematical Modelling and Numerical Analysis
www.esaim-m2an.org

ELLIPTIC INTERFACE PROBLEM APPROXIMATED BY CUTFEM: II. *A POSTERIORI* ERROR ANALYSIS BASED ON EQUILIBRATED FLUXES

Daniela Capatina* and Aimene Gouasmi

Abstract. This paper investigates an elliptic interface problem with discontinuous diffusion coefficients discretized by finite elements on unfitted meshes, employing the cut finite element method (CutFEM). The main contribution is the *a posteriori* error analysis based on equilibrated fluxes belonging to the immersed Raviart–Thomas space. We establish sharp reliability and local efficiency of a new error estimator, which includes both volume and interface terms, carefully tracking the dependence of the efficiency constant on the diffusion coefficients and the mesh/interface configuration. Numerical results highlight the robustness of the approach.

Mathematics Subject Classification. 65N15, 65N30, 65N50.

Received July 11, 2025. Revised April 24, 2026. Accepted May 04, 2026.

1. Introduction

The study of *a posteriori* error estimation for finite element methods has been an active area of research for several decades, as demonstrated by the extensive literature on the topic (see, *e.g.*, [2, 12, 21] and many others). This technique is particularly valuable in adaptive mesh refinement (AMR) procedures, commonly employed for problems with singularities, discontinuities, or sharp derivatives. The *a posteriori* analysis quantifies the error incurred and provides guidance on how to improve the accuracy of the solutions [21]. Several types of *a posteriori* error estimators exist, such as those based on the residuals of the governing differential equations or those based on equilibrated fluxes, which generally yield sharp reliability bounds. Various flux-based *a posteriori* estimators for different finite element methods have been studied by many researchers, see, for example, [1–4, 7, 11, 14, 18, 19, 22, 23]. Using a partition of unity, the pioneering work of Ladevèze and Leguillon [18] introduced a local strategy that reduces the construction of equilibrated fluxes to vertex-patch computations. For the P^1-continuous finite element approximation of the Poisson equation, an equilibrated flux in the lowest-order Raviart–Thomas space was explicitly built in [4, 11] and via local corrections in the broken Raviart–Thomas space. However, this approach does not yield a robust equilibrated estimator with respect to coefficient jumps unless a constrained minimization is introduced; see [7]. In [14], a unified partition-of-unity method was developed, requiring the solution of local mixed problems on each vertex patch. As an exception to partition-of-unity-based approaches, we refer to [3] for a Poisson problem.

Keywords and phrases. A posteriori error analysis, CutFEM, adaptive mesh refinement, unfitted meshes, immersed Raviart–Thomas space.

LMAP CNRS UMR 5142, University of Pau and Pays de l'Adour, 64013 Pau, France
*Corresponding author: daniela.capatina@univ-pau.fr

We consider here a finite element approximation of an elliptic interface problem on unfitted meshes, where the interface Γ is taken into account by the CutFEM method [5, 6]. In [9], we have defined a locally conservative flux belonging to an immersed Raviart–Thomas space (cf. [16]), following the approach developed in [8] for fitted meshes. We have also introduced a global error estimator consisting of a standard term η—the weighted L^2-norm of the difference between the equilibrated and numerical fluxes—plus a new interface term η_Γ, accounting for discontinuities of the discrete solution across the interface and of the equilibrated flux across the cut edges. In this paper, we provide a detailed *a posteriori* error analysis based on this estimator, establishing its robust reliability and local efficiency. To the best of our knowledge, these topics are largely unexplored in the context of CutFEM for interface problems. An *a posteriori* error analysis based on conservative fluxes was carried out in [10] for CutFEM solutions of a Poisson boundary problem on unfitted meshes, but the challenges and techniques required for interface problems are more involved.

We first establish the robust reliability and bound the weighted H^1 semi-norm of the error by the global estimator $\eta + \eta_\Gamma$. The reliability constant of η is equal to 1, in agreement with well-known results for equilibrated flux-based estimators, while the constant in front of η_Γ and the higher-order term is independent of the mesh size, the diffusion coefficients and the mesh/interface geometry. The proof requires introducing a continuous approximation of the CutFEM solution such that the corresponding interpolation error is bounded by the interface estimator η_Γ.

Then, we focus on the proof of the local efficiency for each of the three local error indicators, aiming to obtain the best possible constants with respect to the various parameters. The treatment of the cut cells is challenging, since the difference between the equilibrated and the numerical fluxes is only piecewise Raviart–Thomas. Therefore, we first investigate this space and construct specific basis functions, in relation to the immersed Raviart–Thomas space [16]. Their estimates allow us to bound the flux-based indicators by the residual ones; by adapting the Verfürth argument [21] to the cut cells, we are next able to establish the efficiency, with constants that depend explicitly on the ratio of the diffusion coefficients and the mesh/interface geometry.

Finally, we carry out some numerical tests. The AMR is validated in [9]; therefore, we focus here on illustrating the estimator's behavior. We numerically observe that η_Γ has only a minor influence and can therefore be neglected in the mesh refinement, and that the estimator is robust with respect to the various parameters.

The paper is organized as follows. In Section 2, we give the continuous and discrete formulations, while in Section 3, the equilibrated flux and the *a posteriori* error estimator introduced in [9] are recalled. Section 4 is devoted to the proof of the reliability bound. In the next two sections, we establish some results useful to prove the efficiency: Section 5 is dedicated to the properties of a piecewise Raviart–Thomas space on the cut cells, while in Section 6 the decomposition of the flux correction in the previous space is obtained. Then, we establish the local efficiency in Section 7. Finally, several numerical experiments are presented in Section 8.

2. Continuous and discrete problems

The model problem is given by

$$\begin{cases} -\mathrm{div}(K\nabla u_i) = f & \text{in } \Omega^i \quad (i=1,2), \\ u = 0 & \text{on } \partial\Omega, \\ [u] = 0, \quad [K\nabla u \cdot n_\Gamma] = g & \text{on } \Gamma. \end{cases} \tag{1}$$

where Ω is a two-dimensional polygonal domain and Γ a sufficiently smooth interface, separating Ω into two disjoint subdomains Ω^1 and Ω^2. We denote by n_Γ the unit normal vector to Γ oriented from Ω^1 to Ω^2; the jumps across Γ are defined by $[u] = u_1 - u_2$, where $u_{|\Omega^i} = u_i$. We suppose $f \in L^2(\Omega)$, $g \in L^2(\Gamma)$, and, for the sake of simplicity, we assume $K_{|\Omega^i} = K_i = k_i I$ with $k_i > 0$ for $i = 1, 2$. We consider the following well-posed variational formulation: Find $u \in H_0^1(\Omega)$ such that

$$\int_\Omega K\nabla u \cdot \nabla v \,\mathrm{d}x = \int_\Omega f v \,\mathrm{d}x + \int_\Gamma g v \,\mathrm{d}s, \quad \forall v \in H_0^1(\Omega). \tag{2}$$

In view of the numerical approximation of (2) by the CutFEM method [6], we introduce some notation (see also [9]). Let $\mathcal{T}_h$ be a regular triangular mesh of Ω, whose elements are closed sets, $\mathcal{F}_h$ the set of edges, and h_T and h_F the diameter of $T \in \mathcal{T}_h$ and $F \in \mathcal{F}_h$, respectively. The shape regularity of the triangles is implicitly used in several places in the manuscript. For an interior edge F, n_F is a fixed unit normal vector, oriented from T_F^- to T_F^+ (the two triangles that share F). If $F \subset \partial\Omega$, then n_F is the outward normal vector to Ω, while if $F \subset \Gamma$, then $n_F = n_\Gamma$. For $i = 1, 2$, we define

$$\mathcal{T}_h^i = \left\{T \in \mathcal{T}_h;\ T \cap \Omega^i \neq \emptyset\right\}, \quad \mathcal{F}_h^i = \left\{F \in \mathcal{F}_h;\ F \cap \Omega^i \neq \emptyset\right\}, \quad \Omega_h^i = \bigcup_{T \in \mathcal{T}_h^i} T.$$

For $T \in \mathcal{T}_h$ and $F \in \mathcal{F}_h$, let us define the patches $\Delta_T = \bigcup_{N \in \mathcal{N}_T} \omega_N$ and $\Delta_F = \bigcup_{T,\, \partial T \supset F} \Delta_T$, where $\mathcal{N}_T$ denotes the set of vertices of T and ω_N the set of triangles sharing the node N. As regards the cut elements, let

$$\begin{gathered}\mathcal{T}_h^\Gamma = \{T \in \mathcal{T}_h;\ \mathring{T} \cap \Gamma \neq \emptyset\}, \quad \mathcal{F}_h^\Gamma = \{F \in \mathcal{F}_h;\ \mathring{F} \cap \Gamma \neq \emptyset\},\\ T^i = T \cap \Omega^i \quad \forall T \in \mathcal{T}_h^\Gamma, \quad F^i = F \cap \Omega^i \quad \forall F \in \mathcal{F}_h^\Gamma.\end{gathered}$$

The triangles T of $\mathcal{T}_h$ such that $T \cap \Gamma$ is a single vertex or a whole side of T are treated like non-cut elements.

To focus on the *a posteriori* error analysis based on the new flux, we neglect in this paper the interface approximation error and we assume that Γ is a polygonal line, such that for each $T \in \mathcal{T}_h^\Gamma$, the intersection $\Gamma_T := T \cap \Gamma$ is a segment. We do not allow for interface corners inside an element; in such a situation, the triangle should be split into two sub-triangles, so that Γ_T becomes a segment in each one.

For a function v, sufficiently smooth on each Ω^i but discontinuous across Γ, we denote by $v_i := v_{|\Omega^i}$ and define (cf. [13]) the two following means on Γ:

$$\{v\} = \omega_1 v_1 + \omega_2 v_2, \quad \{v\}^* = \omega_2 v_1 + \omega_1 v_2, \quad \text{with} \quad \omega_1 = \frac{k_2}{k_2 + k_1}, \quad \omega_2 = \frac{k_1}{k_1 + k_2}.$$

It is also useful to introduce the harmonic mean $k_\Gamma = k_1 k_2/(k_1 + k_2)$. Furthermore, we introduce the arithmetic mean and the jump across an interior edge F as follows:

$$\langle v \rangle = \frac{1}{2}(v^- + v^+), \quad [\![v]\!] = v^- - v^+, \quad [\![\partial_n v]\!] = [\![\nabla v]\!] \cdot n_F.$$

For boundary edges, we set $\langle v \rangle = [\![v]\!] = v$. We use the symbols $\lesssim$ and $\approx$ to indicate the existence of generic constants that are independent of the mesh size, the interface geometry, and the diffusion coefficients. Finally, we recall the following trace inequality on a cut element $T \in \mathcal{T}_h^\Gamma$:

$$\forall v \in H^1(T), \quad \|v\|_{\Gamma_T}^2 \lesssim \left(h_T^{-1}\|v\|_T^2 + h_T\|\nabla v\|_T^2\right). \tag{3}$$

The CutFEM approximation of (2) reads: Find $u_h = (u_{h,1}, u_{h,2}) \in \mathcal{C}_h^1 \times \mathcal{C}_h^2$ such that

$$a_h(u_h, v_h) = l_h(v_h) \quad \forall\, v_h \in \mathcal{C}_h^1 \times \mathcal{C}_h^2, \tag{4}$$

where $\mathcal{C}_h^i = \left\{v \in H^1(\Omega_h^i);\ v_{|(\partial\Omega^i \setminus \Gamma)} = 0,\ v_{|T} \in P^1(T),\ \forall\, T \in \mathcal{T}_h^i\right\}$ for $i = 1, 2$ and

$$\begin{aligned} a_h(u_h, v_h) &= \sum_{i=1}^{2}\left(\sum_{T \in \mathcal{T}_h^i}\int_{T^i} k_i \nabla u_{h,i} \cdot \nabla v_{h,i}\, \mathrm{d}x + \gamma_g j_i(u_{h,i}, v_{h,i})\right) + a_\Gamma(u_h, v_h),\\ j_i(u_{h,i}, v_{h,i}) &= \sum_{F \in \mathcal{F}_g^i} h_F \int_F k_i [\![\partial_n u_{h,i}]\!][\![\partial_n v_{h,i}]\!]\, \mathrm{d}s \quad (i = 1,\ 2), \end{aligned}$$

$$a_\Gamma(u_h, v_h) = \sum_{T\in\mathcal{T}_h^\Gamma} \int_{\Gamma_T} \left(\frac{\gamma k_\Gamma}{h_T}[u_h][v_h] - \{K\nabla u_h\cdot n_\Gamma\}[v_h] - \{K\nabla v_h\cdot n_\Gamma\}[u_h] \right) \mathrm{d}s,$$

$$l_h(v_h) = \sum_{i=1}^{2} \int_{\Omega^i} f v_{h,i}\,\mathrm{d}x + \sum_{T\in\mathcal{T}_h^\Gamma} \int_{\Gamma_T} g\{v_h\}^*\,\mathrm{d}s.$$

Here above, $\gamma > 0$ and $\gamma_g > 0$ are stabilization parameters, independent of the mesh, the interface, and the diffusion coefficients, while $\mathcal{F}_g^i = \left\{F\in\mathcal{F}_h^i;\ (T_F^+\cup T_F^-)\cap\Gamma\neq\emptyset\right\}$.

It is well known that for γ large enough, the discrete problem (4) is well-posed.

It is useful to introduce the following norms, for any $v_h\in\mathcal{C}_h^1\times\mathcal{C}_h^2$:

$$|v_h|_{1,K,h}^2 = \sum_{i=1}^{2} \|k_i^{1/2}\nabla v_{h,i}\|_{\Omega^i}^2, \quad \|v_h\|_h^2 = |v_h|_{1,K,h}^2 + \sum_{i=1}^{2} j_i(v_{h,i}, v_{h,i}) + \sum_{T\in\mathcal{T}_h^\Gamma} \frac{k_\Gamma}{h_T}\|[v_h]\|_{\Gamma_T}^2,$$

where $\|\cdot\|_\omega$ is the L^2-norm on $\omega\subset\mathbb{R}^d$ $(1\le d\le 2)$. Let the local semi-norms on $T\in\mathcal{T}_h$ and Δ_T:

$$|v_h|_{1,K,T}^2 = \sum_{i=1}^{2} \|k_i^{1/2}\nabla v_{h,i}\|_{T^i}^2, \quad j_{i,\Delta_T}(v_{h,i}, v_{h,i}) := \sum_{T'\in\Delta_T} \sum_{F\in\mathcal{F}_g^i\cap\mathcal{F}_{T'}} h_F k_i \int_F [\![\partial_n v_{h,i}]\!]^2\,\mathrm{d}s,$$

which can also be defined on any subset $\omega\subset\Omega$ that is a union of cells. Here above, $\mathcal{F}_T$ is the set of sides of T.

In [9], an equivalent hybrid mixed formulation of (4) was proposed and studied. We recall below the definition of its Lagrange multiplier $\theta_h = (\theta_{h,1}, \theta_{h,2})$, which was further used to reconstruct an equilibrated flux. For this purpose, let the spaces be defined as follows:

$$\mathcal{D}_h^i = \{v\in L^2(\mathcal{T}_h^i);\ v_{|T}\in P^1(T)\ \forall T\in\mathcal{T}_h^i\} \quad (i=1,2),$$
$$\mathcal{M}_h^i = \left\{\mu\in L^2(\mathcal{F}_h^i); \mu_{|F}\in P^1(F)\,\forall F\in\mathcal{F}_h^i,\ \sum_{F\in\mathcal{F}_N} \mathfrak{s}_N^F h_F \mu_{|F}(N) = 0\ \forall N\in\overset{\circ}{\mathcal{N}_h^i}\right\},$$

where $\overset{\circ}{\mathcal{N}_h^i}$ denotes the set of nodes interior to Ω_h^i, $\mathcal{F}_N$ the set of edges sharing the node N, and $\mathfrak{s}_N^F = \mathrm{sign}(n_F, N)$ is equal to $1(-1)$ if the orientation of n_F with respect to the node N is in clockwise (counter-clockwise) rotation. Let also the bilinear form

$$b_h(\mu_h, v_h) = \sum_{i=1}^{2} \sum_{F\in\mathcal{F}_h^i} \frac{k_i h_F}{2} \sum_{N\in\mathcal{N}_F} \mu_{h,i|F}(N)[\![v_{h,i}]\!](N), \quad \forall\,\mu_h\in\mathcal{M}_h^1\times\mathcal{M}_h^2,\ v_h\in\mathcal{D}_h^1\times\mathcal{D}_h^2,$$

where $\mathcal{N}_F$ is the set of vertices of the edge F.

Then, we consider the following problem: Find $\theta_h = (\theta_{h,1}, \theta_{h,2})\in\mathcal{M}_h^1\times\mathcal{M}_h^2$ s.t.

$$b_h(\theta_h, v_h) = l_h(v_h) - a_h(u_h, v_h) + \sum_{i=1}^{2} \sum_{F\in\mathcal{F}_h^i} \int_{F^i} \langle k_i\nabla u_{h,i}\cdot n_F\rangle[\![v_{h,i}]\!]\,\mathrm{d}s \quad \forall\, v_h\in\mathcal{D}_h^1\times\mathcal{D}_h^2.$$

It was shown in [9] that it has a unique solution, which can be computed locally as sum of contributions θ_N^i defined on the patches $\omega_N^i = \omega_N\cap\mathcal{T}_h^i$ associated to the nodes N of $\mathcal{T}_h^i$: $\theta_{h,i} = \sum_{N\in\mathcal{N}_h^i}\theta_N^i$ for $1\le i\le 2$. More precisely, $\theta_{h,i}$ belongs to $\mathcal{M}_h^i$, lives on the sides of $\mathcal{F}_N \cap \mathcal{F}_h^i$, and is the unique solution of a small linear system associated to N (see [9] for details). In addition, we have the next bound (see Theorem 2.6 of [9]):

Lemma 2.1. *For $i = 1, 2$ and any node N of $\mathcal{T}_h^i$, we have*

$$\Big(\sum_{F \in \mathcal{F}_N \cap \mathcal{F}_h^i} h_F k_i^2 \|\theta_N^i\|_F^2 \Big)^{1/2} \lesssim \sum_{T \in \omega_N^i} \sqrt{h_T} k_i \left(\|[\![\partial_n u_{h,i}]\!]\|_{\partial T \setminus \partial \omega_N^i} + \|[\![\partial_n u_{h,i}]\!]\|_{\partial T \cap \mathcal{F}_g^i} \right) + \sum_{T \in \mathcal{T}_h^\Gamma \cap \omega_N^i} \left(\frac{k_\Gamma}{\sqrt{h_T}} \|[u_h]\|_{\Gamma_T} + \sqrt{h_T} \|g - [K \nabla u_h \cdot n_\Gamma]\|_{\Gamma_T} \right) + \sum_{T \in \omega_N^i} h_T \|f\|_{T^i}.$$

3. Definition of the flux and the a posteriori error estimators

For the sake of simplicity, we assume from now on $g = 0$, but the study can be extended to nonhomogeneous transmission conditions. We recall that the lowest-order Raviart–Thomas space is defined as $\mathcal{RT}^0(\mathbb{R}^2) = \{(ax_1 + b, ax_2 + c);\, a, b, c \in \mathbb{R}\}$, where $x = (x_1, x_2) \in \mathbb{R}^2$. For $\omega \subset \mathbb{R}^2$, we set $\mathcal{RT}^0(\omega) = \{\psi_{|\omega};\, \psi \in \mathcal{RT}^0(\mathbb{R}^2)\}$.

In [9], an equilibrated conservative flux σ_h was defined in the immersed Raviart–Thomas space $\mathcal{IRT}^0(\mathcal{T}_h)$ of [16]. We recall that on a cut cell T, the elements of this immersed space are piecewise $\mathcal{RT}^0$-functions ψ satisfying

$$[\psi \cdot n_\Gamma] = 0, \quad [K^{-1} \psi \cdot t_\Gamma](x_\Gamma) = 0, \quad \operatorname{div}(\psi_{|T^1}) = \operatorname{div}(\psi_{|T^2}),$$

where x_Γ is an arbitrary point of Γ_T. On any $T \in \mathcal{T}_h$, the local degrees of freedom are the same as for the standard $\mathcal{RT}^0$-space, that is,

$$N_{T,j}(\psi) = \frac{1}{|F_j|} \int_{F_j} \psi \cdot n_T \, \mathrm{d}s \quad (1 \le j \le 3), \tag{5}$$

where $(F_j)_{1 \le j \le 3}$ denote the edges of T and n_T is the outward unit normal vector to T. The recovered flux $\sigma_h \in \mathcal{IRT}^0(\mathcal{T}_h)$ of [9] is defined by imposing its degrees of freedom as follows:

$$\sigma_h \cdot n_F = \langle k_i \nabla u_{h,i} \cdot n_F \rangle - k_i \pi_F^0 \theta_{h,i}, \quad \forall F \in \mathcal{F}_h^i \backslash \mathcal{F}_h^\Gamma \quad (i = 1, 2),$$
$$\int_F \sigma_h \cdot n_F \, \mathrm{d}s = \sum_{i=1}^2 \left(\int_{F^i} \langle k_i \nabla u_{h,i} \cdot n_F \rangle \, \mathrm{d}s - \int_F k_i \theta_{h,i} \, \mathrm{d}s \right), \quad \forall F \in \mathcal{F}_h^\Gamma,$$

where π_F^0 denotes the $L^2(F)$-orthogonal projection on $P^0(F)$. The definition of the degrees of freedom of the immersed Raviart–Thomas space $\mathcal{IRT}^O$ yields that $\int_F [\![\sigma_h \cdot n_F]\!] \, \mathrm{d}s = 0$ on any interior side F, that is, $\pi_0^F [\![\sigma_h \cdot n_F]\!] = 0$. It was proved in Theorem 3.1 of [9] that $\operatorname{div} \sigma_h = -f_h$, with $(f_h)_{|T} = \pi_T^0 f$ for any $T \in \mathcal{T}_h$ and π_T^0 the $L^2(T)$-orthogonal projection on $P^0(T)$.

We next set $\tau_h = K^{-1/2}(\sigma_h - K \nabla_h u_h)$ and define the local error estimator:

$$\eta_T = \|K^{-1/2}(\sigma_h - K \nabla_h u_h)\|_T = \|\tau_h\|_T, \quad \forall T \in \mathcal{T}_h.$$

Since u_h is discontinuous across Γ, we use the discrete gradient ∇_h in a cut triangle $T \in \mathcal{T}_h^\Gamma$; thus, $\nabla_h u_h \in L^2(T)$ is defined by $(\nabla_h u_h)_{|T \cap \Omega^i} = (\nabla u_{h,i})_{|T \cap \Omega^i}$ for $i = 1, 2$.

In addition, on the cut cells $T \in \mathcal{T}_h^\Gamma$ and cut edges $F \in \mathcal{F}_h^\Gamma$, we also consider

$$\tilde{\eta}_T = \frac{\sqrt{h_T k_\Gamma}}{\sqrt{h_T^{\min} |\Gamma_T|}} \|[u_h]\|_{\Gamma_T}, \quad \eta_F = \frac{\sqrt{h_F}}{\sqrt{k_\Gamma}} \|[\![\sigma_h \cdot n_F]\!]\|_F,$$

where $h_T^{\min} = \min\{|F^i|;\ F \in \partial T \cap \mathcal{F}_h^\Gamma,\ i = 1,2\}$.

The global error estimator is given by $\eta + \eta_\Gamma$, where

$$\eta = \left(\sum_{T \in \mathcal{T}_h} \eta_T^2 \right)^{1/2}, \quad \eta_\Gamma = \left(\sum_{F \in \mathcal{F}_h^\Gamma} \eta_F^2 + \sum_{T \in \mathcal{T}_h^\Gamma} \tilde{\eta}_T^2 \right)^{1/2}.$$

The data approximation terms on a triangle $T \in \mathcal{T}_h$ and on Ω are, respectively, given by

$$\epsilon(T) = \frac{h_T}{\sqrt{\delta_T}} \|f - f_h\|_T, \quad \epsilon(\Omega) = \left(\sum_{T \in \mathcal{T}_h} \epsilon(T)^2 \right)^{1/2}, \quad \text{where} \quad \delta_T = \begin{cases} k_i & \text{if } T \in \mathcal{T}_h^i \backslash \mathcal{T}_h^\Gamma \\ k_\Gamma & \text{if } T \in \mathcal{T}_h^\Gamma \end{cases}.$$

We similarly define $\epsilon(\omega)$ on any subset $\omega \subset \Omega$ that is a union of cells. In the following, we establish the reliability and local efficiency of $\eta + \eta_\Gamma$.

4. Reliability

Thanks to the fact that σ_h strongly satisfies the transmission condition, we are able to establish the reliability of the error estimator $\eta + \eta_\Gamma$. As expected, when using equilibrated fluxes in *a posteriori* error estimation, we show that the constant in front of the main part $\eta = \|\tau_h\|_\Omega$ of the global estimator is equal to 1.

The proof is done in three main steps.

4.1. Sharp upper bound of the error

We begin by establishing a sharp bound for the energy norm of the error. However, at this stage, the upper bound is not yet the global estimator $\eta + \eta_\Gamma$.

Lemma 4.1. *There exists a constant $C > 0$ independent of the discretization, the diffusion coefficients, and the interface such that*

$$|u - u_h|_{1,K,h} \le \eta + \inf_{v \in H_0^1(\Omega)} |v - u_h|_{1,K,h} + C \left(\sum_{F \in \mathcal{F}_h^\Gamma} \eta_F^2 + \epsilon(\Omega)^2 \right)^{1/2}.$$

Proof. We consider $\varphi \in H_0^1(\Omega)$, the unique solution of the following weak problem:

$$\int_\Omega K \nabla \varphi \cdot \nabla v \,\mathrm{d}x = \int_\Omega K \nabla_h u_h \cdot \nabla v \,\mathrm{d}x \quad \forall\, v \in H_0^1(\Omega). \tag{6}$$

The triangle inequality gives

$$|u - u_h|_{1,K,h} \le |u - \varphi|_{1,K,h} + |\varphi - u_h|_{1,K,h}. \tag{7}$$

The auxiliary problem (6) immediately yields

$$|\varphi - u_h|_{1,K,h} = \inf_{v \in H_0^1(\Omega)} |v - u_h|_{1,K,h}. \tag{8}$$

With $\sigma = K\nabla u$ and $\tau_h = K^{-1/2}(\sigma_h - K\nabla_h u_h)$, we have

$$\begin{aligned}|u-\varphi|^2_{1,K,h} &= \int_\Omega K^{1/2}\nabla(u-\varphi)\cdot(K^{-1/2}\sigma - K^{-1/2}\sigma_h + \tau_h + K^{1/2}(\nabla_h u_h - \nabla\varphi))\,\mathrm{d}x \\ &= \int_\Omega \nabla(u-\varphi)\cdot(\sigma-\sigma_h)\,\mathrm{d}x + \int_\Omega K^{1/2}\nabla(u-\varphi)\cdot\tau_h\,\mathrm{d}x + \int_\Omega K\nabla(u-\varphi)\cdot(\nabla_h u_h - \nabla\varphi)\,\mathrm{d}x.\end{aligned}$$

The last term in the above equality vanishes thanks to (6). Recalling that $\eta = \|\tau_h\|_\Omega$, the Cauchy–Schwarz inequality then yields

$$|u-\varphi|^2_{1,K,h} \le \left|\int_\Omega \nabla(u-\varphi)\cdot(\sigma-\sigma_h)\,\mathrm{d}x\right| + \eta|u-\varphi|_{1,K,h}. \tag{9}$$

Integrating by parts and using that $(u-\varphi)\in H^1_0(\Omega)$, $\sigma\in H(\mathrm{div},\Omega)$, $[\![\sigma_h\cdot n_F]\!]=0$ on any non-cut interior edge F and $\mathrm{div}\sigma_h = -f_h$, we further obtain

$$\int_\Omega \nabla(u-\varphi)\cdot(\sigma-\sigma_h)\,\mathrm{d}x = \int_\Omega (f-f_h)(u-\varphi)\,\mathrm{d}x - \sum_{F\in\mathcal{F}_h^\Gamma}\int_F [\![\sigma_h\cdot n_F]\!](u-\varphi)\,\mathrm{d}s. \tag{10}$$

Using the Cauchy–Schwarz inequality, $\|u-\varphi-\pi^0_T(u-\varphi)\|_T \lesssim h_T\|\nabla(u-\varphi)\|_T$ for any $T\in\mathcal{T}_h$ and $k_\Gamma\le k_i$ for $i=1,2$, we obtain in a standard way

$$\begin{aligned}\left|\int_\Omega (f-f_h)(u-\varphi)\,\mathrm{d}x\right| &= \left|\sum_{T\in\mathcal{T}_h}\int_T (f-f_h)(u-\varphi-\pi^0_T(u-\varphi))\,\mathrm{d}x\right| \\ &\lesssim \sum_{i=1}^2\sum_{T\in\mathcal{T}_h^i\setminus\mathcal{T}_h^\Gamma}\frac{h_T}{\sqrt{k_i}}\|f-f_h\|_T\|k_i^{1/2}\nabla(u-\varphi)\|_T \\ &\quad + \sum_{T\in\mathcal{T}_h^\Gamma}\frac{h_T}{\sqrt{k_\Gamma}}\|f-f_h\|_T\|k_\Gamma^{1/2}\nabla(u-\varphi)\|_T \\ &\lesssim |u-\varphi|_{1,K,h}\,\epsilon(\Omega).\end{aligned} \tag{11}$$

Let $F\in\mathcal{F}_h^\Gamma$. By definition of the space $\mathcal{IRT}^0$, we have $\pi^0_F[\![\sigma_h\cdot n_F]\!]=0$, hence

$$\left|\sum_{F\in\mathcal{F}_h^\Gamma}\int_F [\![\sigma_h\cdot n_F]\!](u-\varphi)\,\mathrm{d}s\right| \le \sum_{F\in\mathcal{F}_h^\Gamma}\frac{\sqrt{h_F}}{\sqrt{k_\Gamma}}\|[\![\sigma_h\cdot n_F]\!]\|_F\frac{\sqrt{k_\Gamma}}{\sqrt{h_F}}\|u-\varphi-\pi^0_F(u-\varphi)\|_F.$$

We have $h_F^{-1/2}\|u-\varphi-\pi^0_F(u-\varphi)\|_F \lesssim |u-\varphi|_{1,T_F^+\cup T_F^-}$. The proof of this bound is standard: we first use the minimal distance property of π^0_F, which yields $\|u-\varphi-\pi^0_F(u-\varphi)\|_F \le \|u-\varphi-\pi^0_T(u-\varphi)\|_F$ for any triangle T such that $F\subset\partial T$, then the well-known trace inequality $h_F^{-1/2}\|v\|_F \lesssim h_T^{-1}\|v\|_T + |v|_{1,T}$ for any $v\in H^1(T)$, the fact that $|u-\varphi-\pi^0_T(u-\varphi)|_{1,T} = |u-\varphi|_{1,T}$ and finally, the interpolation error estimate $\|u-\varphi-\pi^0_T(u-\varphi)\|_T \lesssim h_T|u-\varphi|_{1,T}$. Next, using the Cauchy–Schwarz inequality and $k_\Gamma\le k_i$ for $i=1,2$, we obtain

$$\left|\sum_{F\in\mathcal{F}_h^\Gamma}\int_F [\![\sigma_h\cdot n_F]\!](u-\varphi)\,\mathrm{d}s\right| \lesssim |u-\varphi|_{1,K,h}\left(\sum_{F\in\mathcal{F}_h^\Gamma}\eta_F^2\right)^{1/2}. \tag{12}$$

Gathering together (9)–(11) and (12), we obtain the following bound:

$$|u-\varphi|_{1,K,h} \leq \eta + C\left(\sum_{F\in\mathcal{F}_h^\Gamma} \eta_F^2 + \epsilon(\Omega)^2\right)^{1/2},$$

which together with (7) and (8) ends the proof. □

Note that

$$\inf_{v\in H_0^1(\Omega)} |v-u_h|_{1,K,h} \leq |I_h u_h - u_h|_{1,K,h} \tag{13}$$

for any interpolation $I_h u_h$ of u_h belonging to $H_0^1(\Omega)$. Therefore, the next step consists of constructing $I_h u_h \in H_0^1(\Omega)$ such that the interpolation error is bounded by η_Γ.

4.2. A continuous approximation of the CutFEM solution

We focus on the cut triangles since on $T \in \mathcal{T}_h \backslash \mathcal{T}_h^\Gamma$, we simply take $I_h u_h = u_h$.

Let $T \in \mathcal{T}_h^\Gamma$. We denote the triangle T by $\triangle A_1A_2A_3$ and let $M \in A_1A_2$, $N \in A_1A_3$ be the intersection points with Γ. The case where T is cut at one of its vertices into two sub-triangles can be treated in a similar manner and leads to analogous results (see Remark 1). Therefore, in what follows, we only detail the case where one of the cut parts is quadrilateral, which is more challenging.

For simplicity of notation, let $T^\triangle$ and $T^\square$ denote the triangular and quadrilateral parts of T, respectively, and assume that $T^\triangle = T^1$, $T^\square = T^2$. Since the ratios $|A_2M|/|A_3N|$ and $|A_3N|/|A_2M|$ cannot blow up simultaneously, we assume, without loss of generality, that $|A_2M|/|A_3N|$ is bounded and then cut $T^\square$ into two triangles using A_3M, cf. Figure 1(a) (otherwise, use A_2N). We define the interpolation operator I_h as follows: $I_h u_h$ is a linear function on each sub-triangle $\triangle A_1MN =: T^\triangle$, $\triangle MA_2A_3 =: T_1^\square$, and $\triangle MNA_3 =: T_2^\square$, and

$$I_h u_h(A_1) = u_{h,1}(A_1), \quad I_h u_h(A_2) = u_{h,2}(A_2), \quad I_h u_h(A_3) = u_{h,2}(A_3), \tag{14}$$

$$I_h u_h(M) = \{u_h\}^*(M), \quad I_h u_h(N) = \{u_h\}^*(N). \tag{15}$$

This choice guarantees that $I_h u_h \in H^1(T)$, since it is continuous at the intersection points M, N, and A_3 of the sub-triangles. Since $[\![I_h u_h]\!]_F = 0$ for any edge $F \in \mathcal{F}_h$, we have $I_h u_h \in H_0^1(\Omega)$.

In view of estimating the interpolation error $|I_h u_h - u_h|_{1,K,T}$, we first write it as

$$|I_h u_h - u_h|_{1,K,T}^2 = |I_h u_h - u_{h,1}|_{1,K,T^\triangle}^2 + \sum_{l=1}^{2} |I_h u_h - u_{h,2}|_{1,K,T_l^\square}^2, \tag{16}$$

where for any $\tilde{T} \in \{T^\triangle, T_1^\square, T_2^\square\}$ and any $v \in H^1(\tilde{T})$, we set $|v|_{1,K,\tilde{T}} = \|K^{1/2}\nabla v\|_{\tilde{T}}$. Let now $\tilde{T} \in \{T^\triangle, T_1^\square, T_2^\square\}$ and assume $\tilde{T} \subset \Omega^i$, with $i \in \{1,2\}$. Then, we have, thanks to (14) and (15),

$$(I_h u_h - u_h)_{|\tilde{T}} = (-1)^i \omega_i [u_h](M)\varphi_M + (-1)^i \omega_i [u_h](N)\varphi_N,$$

where $\varphi_M, \varphi_N \in P^1(\tilde{T})$ are the nodal basis functions associated to M and N. We express them below in terms of the barycentric coordinates $(\lambda_j)_{1\leq j\leq 3}$ of T.

Lemma 4.2. *We have*

$$(\varphi_M)_{|T^\triangle} = \frac{|F_3|}{|A_1M|}\lambda_2, \quad (\varphi_N)_{|T^\triangle} = \frac{|F_2|}{|A_1N|}\lambda_3, \tag{17}$$

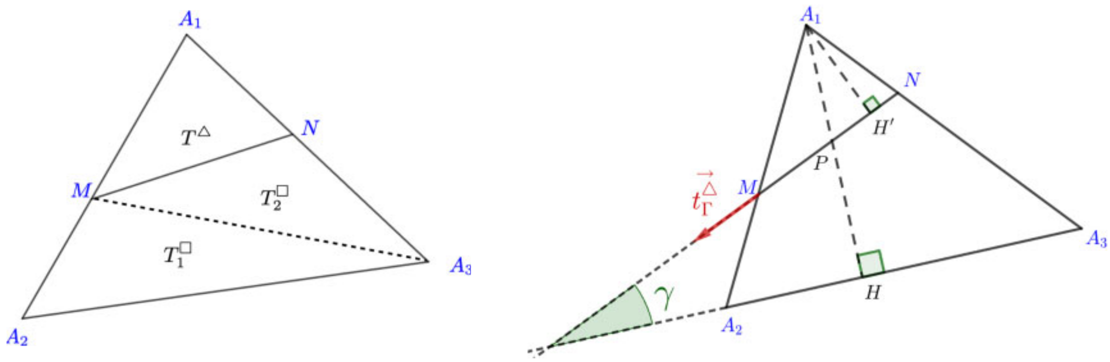

(a) Notation for interpolation (b) Notation for estimate (28)

FIGURE 1. Notation on a cut element.

$$(\varphi_M)_{|T_1^\square} = \frac{|F_3|}{|A_2M|}\lambda_1, \quad (\varphi_N)_{|T_1^\square} = 0, \tag{18}$$

$$(\varphi_M)_{|T_2^\square} = \frac{|F_3|}{|A_1M|}\lambda_2, \quad (\varphi_N)_{|T_2^\square} = \frac{|F_2|}{|A_3N|}\lambda_1 - \frac{|F_2|}{|A_3N|}\frac{|A_2M|}{|A_1M|}\lambda_2, \tag{19}$$

where F_j denotes the edge opposite to the node A_j for $1 \le j \le 3$.

Proof. On $T^\triangle$, we have $\varphi_M(A_1) = \varphi_M(N) = 0$ and $\lambda_{2|F_2} = 0$; therefore, $\varphi_M = c\lambda_2$ with $c \in \mathbb{R}$. From the relation $\lambda_2(M) = |A_1M|/|F_3|$, we obtain the desired expression of $(\varphi_M)_{|T^\triangle}$. We similarly obtain the expression of $(\varphi_N)_{|T^\triangle}$; therefore, (17) is established.

On $T_1^\square$, we immediately obtain $(\varphi_N)_{|T_1^\square} = 0$. The expression of φ_M is obtained in a similar way to the previous case, thus yielding (18). Finally, on $T_2^\square$, we similarly obtain φ_M while φ_N is obtained by decomposing it in the barycentric basis:

$$(\varphi_N)_{|T_2^\square} = a\lambda_1 + b\lambda_2 + c\lambda_3, \quad a, b, c \in \mathbb{R}.$$

From $\varphi_N(A_3) = 0$, we obtain $c = 0$. Moreover, we have $\varphi_N(M) = a\lambda_1(M) + b\lambda_2(M) = 0$ and $\varphi_N(N) = a\lambda_1(N) = 1$. Using next

$$\lambda_1(M) = \frac{|A_2M|}{|F_3|}, \quad \lambda_1(N) = \frac{|A_3N|}{|F_2|}, \quad \lambda_2(M) = \frac{|A_1M|}{|F_3|},$$

we compute a and b and obtain the relation (19). □

4.3. Estimate of the interpolation error

We can now bound the interpolation error $|I_h u_h - u_h|_{1,K,T}$ on any cut triangle T. We begin by establishing an auxiliary estimate. For this purpose, let $\alpha := [u_h](M)$ and $\beta := [u_h](N)$, as well as

$$E_\alpha := \frac{|T^\triangle|}{|A_1M|^2} + \frac{|T_1^\square|}{|A_2M|^2} + \frac{|T_2^\square|}{|A_1M|^2}, \quad E_\beta := \frac{|T^\triangle|}{|A_1N|^2} + \frac{|T_2^\square|}{|A_3N|^2}\frac{|F_3|^2}{|A_1M|^2}. \tag{20}$$

Lemma 4.3. *We have*

$$|I_h u_h - u_h|^2_{1,K,T} \lesssim k_\Gamma(\alpha^2 E_\alpha + \beta^2 E_\beta).$$

Proof. We use (16) and bound the error on each sub-triangle $\tilde{T}$ of T.

First, let $\tilde{T} = T^{\triangle}$. Using $k_\Gamma = k_i\omega_i$ and $0 < \omega_i < 1$ for $i = 1, 2$, we obtain

$$|I_h u_h - u_{h,1}|^2_{1,K,T^{\triangle}} \le k_\Gamma |W_h^{\triangle}|^2_{1,T^{\triangle}}$$

where $W_h^{\triangle}$ belongs to $P^1(T^{\triangle})$ and satisfies $W_h^{\triangle}(M) = -\alpha$, $W_h^{\triangle}(N) = -\beta$, and $W_h^{\triangle}(A_1) = 0$. Hence, $W_h^{\triangle} = -\alpha\varphi_M - \beta\varphi_N$. From (17), combined with the relations,

$$|\lambda_j|^2_{1,T^{\triangle}} = \frac{|T^{\triangle}|}{|T|}|\lambda_j|^2_{1,T}, \quad |\lambda_j|_{1,T} \lesssim 1 \quad (1 \le j \le 3), \quad |T| \approx h_T^2 \tag{21}$$

and $|F_j| \le h_T$ $(1 \le j \le 3)$, we obtain the following bound:

$$|I_h u_h - u_{h,1}|^2_{1,K,T^{\triangle}} \lesssim k_\Gamma \left(\alpha^2 \frac{|T^{\triangle}|}{|A_1 M|^2} + \beta^2 \frac{|T^{\triangle}|}{|A_1 N|^2}\right). \tag{22}$$

Next, let $\tilde{T} = T_1^{\square}$. Similarly, one has $|I_h u_h - u_{h,2}|^2_{1,K,T_1^{\square}} \le k_\Gamma |W_h^1|^2_{1,T_1^{\square}}$, where $W_h^1 \in P^1(T_1^{\square})$ and now satisfies $W_h^1(M) = \alpha$, $W_h^1(A_2) = W_h^1(A_3) = 0$. Hence, $W_h^1 = \alpha\varphi_M$ and from (18) and (21) we obtain

$$|I_h u_h - u_{h,2}|^2_{1,K,T_1^{\square}} \lesssim k_\Gamma \alpha^2 \frac{|T_1^{\square}|}{|A_2 M|^2}. \tag{23}$$

Finally, for $\tilde{T} = T_2^{\square}$, we similarly have

$$|I_h u_h - u_{h,2}|^2_{1,K,T_2^{\square}} \le k_\Gamma |W_h^2|^2_{1,T_2^{\square}}$$

where $W_h^2 \in P^1(T_2^{\square})$ with $W_h^2(M) = \alpha$, $W_h^1(N) = \beta$ and $W_h^2(A_3) = 0$, which yields $W_h^2 = \alpha\varphi_M + \beta\varphi_N$. From (19), we obtain

$$|W_h^2|^2_{1,T_2^{\square}} \lesssim \alpha^2 \frac{|F_3|^2}{|A_1 M|^2}\frac{|T_2^{\square}|}{|T|}|\lambda_2|^2_{1,T} + \beta^2 \frac{|F_2|^2}{|A_3 N|^2}\frac{|T_2^{\square}|}{|T|}\left(|\lambda_1|^2_{1,T} + \frac{|A_2 M|^2}{|A_1 M|^2}|\lambda_2|^2_{1,T}\right).$$

Using again (21), we obtain the following inequality:

$$\frac{|F_2|^2}{|A_3 N|^2}\frac{|T_2^{\square}|}{|T|}\left(|\lambda_1|^2_{1,T} + \frac{|A_2 M|^2}{|A_1 M|^2}|\lambda_2|^2_{1,T}\right) \lesssim \frac{|T_2^{\square}|}{|A_3 N|^2}\left(1 + \frac{|A_2 M|^2}{|A_1 M|^2}\right) \lesssim \frac{|T_2^{\square}|}{|A_3 N|^2}\frac{|F_3|^2}{|A_1 M|^2}.$$

Hence, we finally deduce that

$$|I_h u_h - u_{h,2}|^2_{1,K,T_2^{\square}} \lesssim k_\Gamma \left(\alpha^2 \frac{|T_2^{\square}|}{|A_1 M|^2} + \beta^2 \frac{|T_2^{\square}|}{|A_3 N|^2}\frac{|F_3|^2}{|A_1 M|^2}\right). \tag{24}$$

Gathering together the estimates (22)–(24) in (16) ends the proof. □

The next step consists of bounding the terms E_α and E_β in the best possible way with respect to the geometry of the cut cell T. A first estimate is given in the following lemma, based on equivalent expressions of these terms.

Lemma 4.4. *We have*

$$E_\alpha = \frac{|T|}{|A_1 M||A_2 M|}, \quad E_\beta \le \frac{|T|}{|A_1 N||A_3 N|} + \frac{|T|}{|F_2||A_1 M|}\frac{|A_2 M|}{|A_3 N|}.$$

Proof. We start by developing the expressions of E_α and E_β introduced in (20). For this purpose, it is useful to note that

$$\frac{|T^\triangle|}{|T|} = \frac{|A_1M||A_1N|}{|F_3||F_2|}, \quad \frac{|T_1^\square|}{|T|} = \frac{|A_2M|}{|F_3|}, \quad \frac{|T_2^\square|}{|T|} = 1 - \frac{|T_1^\square|}{|T|} - \frac{|T^\triangle|}{|T|}.$$

Using $|A_1N| + |A_3N| = |F_2|$ and $|A_1M| + |A_2M| = |F_3|$, we further obtain

$$\frac{|T_2^\square|}{|T|} = \frac{|A_1M|}{|F_3|}\left(1 - \frac{|A_1N|}{|F_2|}\right) = \frac{|A_1M|}{|F_3|}\frac{|A_3N|}{|F_2|}.$$

Substituting $|T^\triangle|$, $|T_1^\square|$, and $|T_2^\square|$ from the previous relations in (20), we obtain after some straightforward computation:

$$\begin{aligned} E_\alpha &= |T|\left(\frac{1}{|A_1M||F_3|} + \frac{1}{|A_2M||F_3|}\right) = \frac{|T|}{|A_1M||MA_2|}, \\ E_\beta &= \frac{|T|}{|F_2|}\left(\frac{|A_1M|}{|A_1N||F_3|} + \frac{|F_3|}{|A_1M||A_3N|}\right). \end{aligned}$$

In the expression of E_β, we next use $|A_1M| \le |F_3|$ and substitute $|F_3| = |A_1M| + |A_2M|$ to obtain

$$E_\beta \le \frac{|T|}{|F_2|}\left(\frac{1}{|A_1N|} + \frac{1}{|A_3N|} + \frac{|A_2M|}{|A_1M||A_3N|}\right) = \frac{|T|}{|A_1N||A_3N|} + \frac{|T|}{|F_2||A_1M|}\frac{|A_2M|}{|A_3N|}.$$

This ends the lemma's proof. $\square$

Next, we bound E_α and E_β by a simpler expression.

Lemma 4.5. *We have*

$$E_\alpha \le \frac{h_T}{h_T^{\min}}, \quad E_\beta \lesssim \frac{h_T}{h_T^{\min}}.$$

Proof. Since $|A_1M| + |A_2M| = |F_3|$, we have

$$|A_1M||A_2M| \ge \min\{|A_1M|, |A_2M|\}\frac{|F_3|}{2}.$$

Therefore, from Lemma 4.4 we immediately deduce the bound for E_α:

$$E_\alpha \le \frac{2|T|}{h_T^{\min}|F_3|} \le \frac{h_T}{h_T^{\min}},$$

recalling that $h_T^{\min} = \min\{|A_1M|, |A_2M|, |A_1N|, |A_3N|\}$. Using now $|A_1N| + |A_3N| = |F_2|$, we similarly obtain

$$E_\beta \le \frac{h_T}{h_T^{\min}} + \frac{|T|}{|F_2|h_T^{\min}}\frac{|A_2M|}{|A_3N|} \le \frac{h_T}{h_T^{\min}} + \frac{2h_T}{h_T^{\min}}\frac{|A_2M|}{|A_3N|}.$$

Our initial choice of cutting $T^\square$ into two sub-triangles ensures that $|A_2M|/|A_3N|$ is bounded (otherwise, it suffices to change the roles between M and N). Therefore, we also obtain $E_\beta \lesssim h_T/h_T^{\min}$, which concludes the proof. $\square$

Remark 1. Lemma 4.5 remains unchanged in the case where T is cut by Γ at one of its vertices—let us say $A_3 = N$—into two sub-triangles. One can then choose either of the sub-triangles as T^Δ, let us say $T^\Delta = A_1A_3M$.

Then, we have $\varphi_N = \lambda_3$, $(\varphi_M)_{|T^\triangle} = \frac{|F_3|}{|A_1M|}\lambda_2$, and $(\varphi_M)_{|T^\square} = \frac{|F_3|}{|A_2M|}\lambda_1$. The proofs of Lemmas 4.3–4.5 follow the same idea as in the quadrilateral case, although they are simpler. We thus obtain

$$E_\alpha = 1, \quad E_\beta = \frac{|T^\triangle|}{|A_1M|^2} + \frac{|T^\square|}{|A_2M|^2} \le \frac{h_T}{2}\left(\frac{1}{|A_1M|} + \frac{1}{|A_2M|}\right) = \frac{h_T|F_3|}{2|A_1M||A_2M|} \le \frac{h_T}{h_T^{\min}}.$$

We can now establish the interpolation error estimate in a cut cell.

Lemma 4.6. *Let $T \in \mathcal{T}_h^\Gamma$. Then, one has $|I_h u_h - u_h|_{1,K,T} \lesssim \tilde{\eta}_T$.*

Proof. Lemmas 4.3 and 4.5 yield

$$|I_h u_h - u_h|^2_{1,K,T} \lesssim \frac{h_T k_\Gamma}{h_T^{\min}}(\alpha^2 + \beta^2) \lesssim \frac{h_T k_\Gamma}{h_T^{\min}|\Gamma_T|}\|[u_h]\|^2_{\Gamma_T} = \tilde{\eta}_T^2,$$

which is the desired result. $\square$

By summing the estimate of Lemma 4.6 over the cut cells, we immediately obtain from (13) the next bound.

Lemma 4.7. *We have $\inf\limits_{v \in H_0^1(\Omega)} |v - u_h|_{1,K,h} \lesssim \eta_\Gamma$.*

Finally, thanks to Lemmas 4.1 and 4.7, we deduce the reliability bound.

Theorem 4.8 (Reliability)**.** *There exists a constant $C > 0$ independent of the mesh, the coefficients, and the interface such that*

$$|u - u_h|_{1,K,h} \le \eta + C\left(\eta_\Gamma + \epsilon(\Omega)\right). \tag{25}$$

This theorem shows that the weighted H^1 semi-norm of the error is bounded by the global estimator $\eta + \eta_\Gamma$ plus the higher-order term $\epsilon(\Omega)$, with a reliability constant that is independent of the mesh size, the diffusion coefficients, and the mesh/interface configuration. In addition, the constant in front of the main estimator η is equal to 1, as expected.

Remark 2. The price to pay to obtain a reliability constant independent of the mesh/interface geometry was to weight the estimator $\tilde{\eta}_T$ on a cut triangle by $\sqrt{h_T}/\sqrt{h_T^{\min}}$, which arises from our definition of I_h. Although this factor may become unbounded, it does not seem to influence the estimator's behavior in the numerical tests. If one is able to construct a continuous interpolation $I_h u_h$ of u_h, for which the interpolation error is fully robust with respect to the mesh/interface configuration, then the factor $\sqrt{h_T}/\sqrt{h_T^{\min}}$ would disappear.

5. Properties of a piecewise Raviart–Thomas space on the cut cells

To establish the local efficiency of $\eta_T = \|K^{-1/2}(\sigma_h - K\nabla_h u_h)\|_T$ on a cut triangle $T \in \mathcal{T}_h^\Gamma$, we first need some properties of the finite element space to which $\sigma_h - K\nabla_h u_h$ belongs. Note that although σ_h belongs to the immersed Raviart–Thomas space $\mathcal{IRT}^0(T)$, $\sigma_h - K\nabla_h u_h$ is only piecewise $\mathcal{RT}^0$ on a cut triangle T, that is, its restriction to each part $T^i = T \cap \Omega^i$ belongs to $\mathcal{RT}^0$; this is due to the discontinuity of the diffusion coefficients K and of the approximate solution u_h.

In this section, we provide some properties of this space in relation to the immersed one. In particular, we construct and bound specific shape functions, which will be used in Section 7 to decompose $\sigma_h - K\nabla_h u_h$.

5.1. Auxiliary results

We recall (cf. [20]) the shape functions of the standard Raviart–Thomas space $\mathcal{RT}^0(T)$ on a triangle T of nodes $(A_j)_{1\le j\le 3}$. The basis function $\Lambda_{T,j}$, associated to the edge F_j opposite to A_j, satisfies

$$\Lambda_{T,j}(x) = \frac{|F_j|}{2|T|}\overrightarrow{A_j x}, \quad |\Lambda_{T,j}(x)| \lesssim 1, \quad \|\Lambda_{T,j}\|_T \lesssim h_T \quad (1 \le j \le 3). \tag{26}$$

The local Raviart–Thomas interpolation operator is denoted by I_T.

On a cut triangle $T \in \mathcal{T}_h^\Gamma$, we agree to denote by $n_\Gamma^\triangle$ the unit normal vector to Γ pointing from $T^\triangle$ to $T^\square$ and by $t_\Gamma^\triangle$ the unit tangent vector oriented by a 90° clockwise rotation of $n_\Gamma^\triangle$. We consider the following functions ω and ρ on T:

$$\omega = \begin{cases} t_\Gamma^\triangle & \text{in } T^\triangle \\ 0 & \text{in } T^\square \end{cases}, \quad \rho = \begin{cases} n_\Gamma^\triangle & \text{in } T^\triangle \\ 0 & \text{in } T^\square. \end{cases} \tag{27}$$

The function ω was already introduced in [16], where it was used to prove the unisolvency of $\mathcal{IRT}^0(T)$. It was also shown to satisfy the following bound:

$$0 \le (I_T\omega \cdot t_\Gamma^\triangle)(x) \le 1, \quad \forall x \in T. \tag{28}$$

Remark 3. The bound (28) was established in [16] under the assumption that the cut triangle T is acute. In fact, this assumption is not necessary, as explained below. From Lemma 4.2 of [16] we have, with the notation of Figure 1(b),

$$\forall\, x \in T, \quad (I_T\omega \cdot t_\Gamma^\triangle)(x) = \frac{1}{2|T|}(\overrightarrow{A_3A_2} \cdot t_\Gamma^\triangle)(\overrightarrow{A_1M} \cdot n_\Gamma^\triangle).$$

Using next $\overrightarrow{A_1M} \cdot n_\Gamma^\triangle = |A_1M| \sin(\widehat{A_1MN}) = |A_1H'|$ (with A_1H' the height of $\triangle A_1MN$), $\overrightarrow{A_3A_2} \cdot t_\Gamma^\triangle = |A_3A_2| \cos\gamma$ (with γ the non-oriented angle between $\overrightarrow{NM}$ and $\overrightarrow{A_3A_2}$), and $2|T| = |A_3A_2||A_1H|$ (with A_1H the height of $\triangle A_1A_2A_3$), we obtain

$$\forall x \in T, \quad (I_T\omega \cdot t_\Gamma^\triangle)(x) = \frac{|A_1H'|}{|A_1H|}\cos\gamma.$$

Furthermore, we have $|A_1H'| \le |A_1P| \le |A_1H|$ and $0 \le \gamma \le \frac{\pi}{2}$, which yields (28).

We can easily prove a similar estimate for the new function ρ, which is

$$|(I_T\rho \cdot t_\Gamma^\triangle)(x)| \lesssim 1 \quad \forall\, x \in T. \tag{29}$$

Indeed, thanks to $|\Lambda_{T,j}(x)| \lesssim 1$ and $|\rho(x)| \le 1$ for all $x \in T$, we obtain

$$|(I_T\rho)(x) \cdot t_\Gamma^\triangle| \le \sum_{j=1}^{3} |N_{T,j}(\rho)||\Lambda_{T,j}(x)| \lesssim \sum_{j=1}^{3} \frac{1}{|F_j|}\int_{F_j} |\rho \cdot n_T| \,\mathrm{d}s \lesssim 1.$$

Next, we consider the following functions on the cut triangle T:

$$\phi_t = \omega - I_T\omega, \quad \phi_n = \rho - I_T\rho, \tag{30}$$

which are clearly piecewise $\mathcal{RT}^0$ and satisfy $N_{T,j}(\phi_t) = N_{T,j}(\phi_n) = 0$ for $1 \le j \le 3$. They also satisfy the following properties.

Lemma 5.1. *Let $F_j^{\triangle} = F_j \cap \partial T^{\triangle}$ for $j = 2, 3$. We have*

$$\|\phi_t\|_T \lesssim \sum_{j=2}^{3} |F_j^{\triangle}|, \quad \|\phi_n\|_T \lesssim \sum_{j=2}^{3} |F_j^{\triangle}|.$$

Proof. From the definitions (27) of ω and ρ, we immediately obtain

$$\|\rho\|_T^2 = \|\omega\|_T^2 = |T^{\triangle}| \leq \frac{1}{2}|F_2^{\triangle}||F_3^{\triangle}| \leq \frac{1}{4}\left(\sum_{j=2}^{3}|F_j^{\triangle}|\right)^2. \tag{31}$$

By definition of the Raviart–Thomas interpolation operator I_T, we obtain, thanks to (26),

$$\|I_T\rho\|_T \lesssim h_T \sum_{j=1}^{3} |N_{T,j}(\rho)|, \quad \|I_T\omega\|_T \lesssim h_T \sum_{j=1}^{3} |N_{T,j}(\omega)|,$$

where $N_{T,1}(\rho) = N_{T,1}(\omega) = 0$, and for $2 \leq j \leq 3$, we have

$$\begin{aligned} |N_{T,j}(\rho)| &\leq \frac{1}{|F_j|}\int_{F_j} |\rho \cdot n_T| \, \mathrm{d}s = \frac{1}{|F_j|}\int_{F_j^{\triangle}} |n_\Gamma^{\triangle} \cdot n_T| \, \mathrm{d}s \leq \frac{|F_j^{\triangle}|}{|F_j|}, \\ |N_{T,j}(\omega)| &\leq \frac{1}{|F_j|}\int_{F_j} |\omega \cdot n_T| \, \mathrm{d}s = \frac{1}{|F_j|}\int_{F_j^{\triangle}} |t_\Gamma^{\triangle} \cdot n_T| \, \mathrm{d}s \leq \frac{|F_j^{\triangle}|}{|F_j|}. \end{aligned}$$

Hence, we end up with $\|I_T\omega\|_T \lesssim \sum_{j=2}^{3}|F_j^{\triangle}|$ and $\|I_T\rho\|_T \lesssim \sum_{j=2}^{3}|F_j^{\triangle}|$, which, together with (30) and (31), yield the result. $\square$

It is useful to recall that $\mathrm{div}(\phi_t)$ and $\mathrm{div}(\phi_n)$ are constant on each T^i $(1 \leq i \leq 2)$ and that $[\phi_t \cdot n_\Gamma]$ and $[\phi_n \cdot n_\Gamma]$ are constant on Γ_T, thanks to the properties of the Raviart–Thomas space $\mathcal{RT}^0$; we also recall that x_Γ is the arbitrary point of Γ_T considered in the definition of $\mathcal{IRT}^0(T)$, cf. Section 3.

Lemma 5.2. *Let $T \in \mathcal{T}_h^\Gamma$. We have*

$$\begin{aligned} \mathrm{div}(\phi_{t|T^1}) = \mathrm{div}(\phi_{t|T^2}), \quad [\phi_t \cdot n_\Gamma] = 0, \quad [\phi_t \cdot t_\Gamma](x_\Gamma) = 1, \\ \mathrm{div}(\phi_{n|T^1}) = \mathrm{div}(\phi_{n|T^2}), \quad [\phi_n \cdot n_\Gamma] = 1, \quad [\phi_n \cdot t_\Gamma](x_\Gamma) = 0. \end{aligned}$$

Proof. The relations concerning ϕ_t were already established in [16]. The proof for ϕ_n is similar. Since $\mathrm{div}(I_T\rho)$ is constant on T and ρ is piecewise constant, we obtain the first equality. Then, using that $I_T\rho$ is continuous across Γ_T and that $n_\Gamma^{\triangle} \cdot t_\Gamma = 0$, we obtain the last equality on Γ_T, and in particular at the point x_Γ. Considering then the cases $T^{\triangle} = T^1$ and $T^{\triangle} = T^2$, we also obtain the second relation: $[\phi_n \cdot n_\Gamma] = [\rho \cdot n_\Gamma] = (n_\Gamma^{\triangle} \cdot n_\Gamma)^2 = 1$ on Γ_T. $\square$

Thus, ϕ_t and ϕ_n belong to the following subspace of $\mathcal{RT}^0(T^1) \times \mathcal{RT}^0(T^2)$:

$$\mathcal{E}(T) := \left\{\tau = (\tau_1, \tau_2) \in \mathcal{RT}^0(T^1) \times \mathcal{RT}^0(T^2); \, \mathrm{div}\tau_1 = \mathrm{div}\tau_2\right\}.$$

To conclude this subsection, let us introduce the linear operator $\mathcal{R}_T : \mathcal{E}(T) \longrightarrow \mathbb{R}^5$,

$$\mathcal{R}_T(\tau_1, \tau_2) = \left(\left(\int_{F_j} \tau \cdot n_T \, \mathrm{d}s\right)_{1 \leq j \leq 3}, \, [\tau \cdot n_\Gamma], \, [K^{-1}\tau \cdot t_\Gamma](x_\Gamma)\right).$$

Lemma 5.3. *The operator $\mathcal{R}_T$ is bijective.*

Proof. Since $\dim \mathcal{E}(T) = 5$, it is sufficient to prove that $\mathcal{R}_T$ is injective. Let $\tau = (\tau_1, \tau_2) \in \mathcal{E}(T)$ such that $\mathcal{R}_T(\tau_1, \tau_2) = 0$, that is,

$$\tau_{|T^i} \in \mathcal{RT}^0(T^i), \quad \operatorname{div}(\tau)_{|T^1} = \operatorname{div}(\tau)_{|T^2}, \quad [\tau \cdot n_\Gamma] = 0, \quad [K^{-1}\tau \cdot t_\Gamma](x_\Gamma) = 0,$$

and $N_{T,j}(\tau) = 0$ for $1 \le j \le 3$. However, this implies that $\tau \in \mathcal{IRT}^0(T)$ and the unisolvency of this space immediately yields that $\tau = 0$, whence the result. $\square$

5.2. Construction of specific shape functions

Since $\mathcal{R}_T$ is bijective, there exist unique functions Λ_n and Λ_t in $\mathcal{E}(T)$ such that

$$\mathcal{R}_T(\Lambda_n) = (0,0,0,1,0), \quad \mathcal{R}_T(\Lambda_t) = (0,0,0,0,1). \tag{32}$$

In other words, Λ_n and Λ_t belong to $\mathcal{E}(T)$ and satisfy $N_{T,j}(\Lambda_t) = N_{T,j}(\Lambda_n) = 0$ for $1 \le j \le 3$, as well as

$$\begin{cases} \Lambda_{n|T^i} \in \mathcal{RT}^0(T^i), \quad i = 1,2 \\ \operatorname{div}(\Lambda_{n|T^1}) = \operatorname{div}(\Lambda_{n|T^2}) \\ [\Lambda_n \cdot n_\Gamma] = 1 \\ [K^{-1}\Lambda_n \cdot t_\Gamma](x_\Gamma) = 0 \end{cases}, \quad \begin{cases} \Lambda_{t|T^i} \in \mathcal{RT}^0(T^i), \quad i = 1,2 \\ \operatorname{div}(\Lambda_{t|T^1}) = \operatorname{div}(\Lambda_{t|T^2}) \\ [\Lambda_t \cdot n_\Gamma] = 0 \\ [K^{-1}\Lambda_t \cdot t_\Gamma](x_\Gamma) = 1 \end{cases}. \tag{33}$$

In the sequel, we express Λ_n and Λ_t in terms of the functions ϕ_n and ϕ_t previously introduced in (30). The only difference between ϕ_n, ϕ_t and Λ_n, Λ_t is the presence of the diffusion coefficient K in the jump of the tangential trace.

Lemma 5.4. *Let $k_\triangle := k_{|T^\triangle}$ and $k_\square := k_{|T^\square}$. We have*

$$\Lambda_n = \alpha_n \phi_t + \phi_n, \quad \Lambda_t = \beta_t \phi_t, \tag{34}$$

where

$$\alpha_n = \frac{\left(1 - \frac{k_\triangle}{k_\square}\right)(I_T\rho \cdot t_\Gamma^\triangle)(x_\Gamma)}{A}, \quad \beta_t = \frac{k_\triangle}{A}, \quad A = 1 - \left(1 - \frac{k_\triangle}{k_\square}\right)(I_T\omega \cdot t_\Gamma^\triangle)(x_\Gamma). \tag{35}$$

Proof. Since we already have the existence and uniqueness of Λ_n and Λ_t, we can start from (34) and show that we can uniquely determine the constants α_n and β_t such that Λ_n and Λ_t thus defined satisfy the desired properties (33). Thanks to the properties of ϕ_n and ϕ_t stated in Lemma 5.2, we clearly have $\Lambda_n, \Lambda_t \in \mathcal{E}(T)$, and

$$N_{T,j}(\Lambda_n) = N_{T,j}(\Lambda_t) = 0 \quad (1 \le j \le 3), \quad [\Lambda_n \cdot n_\Gamma] = 1, \quad [\Lambda_t \cdot n_\Gamma] = 0.$$

Next, we look for α_n and β_t such that $[K^{-1}\Lambda_n \cdot t_\Gamma](x_\Gamma) = 0$ and $[K^{-1}\Lambda_t \cdot t_\Gamma](x_\Gamma) = 1$. We first impose

$$0 = [K^{-1}\Lambda_n \cdot t_\Gamma](x_\Gamma) = \alpha_n[K^{-1}\phi_t \cdot t_\Gamma](x_\Gamma) + [K^{-1}\phi_n \cdot t_\Gamma](x_\Gamma). \tag{36}$$

A simple computation yields

$$\begin{aligned} &[K^{-1}\phi_t \cdot t_\Gamma](x_\Gamma) = (K^{-1}\omega \cdot t_\Gamma)_{|T^1}(x_\Gamma) - (K^{-1}\omega \cdot t_\Gamma)_{|T^2}(x_\Gamma) - [K^{-1}](I_T\omega \cdot t_\Gamma)(x_\Gamma), \\ &[K^{-1}\phi_n \cdot t_\Gamma](x_\Gamma) = -[K^{-1}](I_T\rho \cdot t_\Gamma)(x_\Gamma). \end{aligned}$$

Next, we distinguish between two cases, depending on which subdomain contains $T^\triangle$. We define the jump with respect to $n_\Gamma^\triangle$ by $[w]_\triangle = n_\Gamma \cdot n_\Gamma^\triangle [w]$. If $T^\triangle = T^1$, then $t_\Gamma = t_\Gamma^\triangle$, $[K^{-1}] = [K^{-1}]_\triangle = k_\triangle^{-1} - k_\square^{-1}$, and the previous relations become

$$[K^{-1}\phi_t \cdot t_\Gamma] = k_\triangle^{-1} - [K^{-1}]_\triangle I_T\omega \cdot t_\Gamma^\triangle, \quad [K^{-1}\phi_n \cdot t_\Gamma] = -[K^{-1}]_\triangle I_T\rho \cdot t_\Gamma^\triangle. \tag{37}$$

If $T^\triangle = T^2$, then $t_\Gamma = -t_\Gamma^\triangle$, $[K^{-1}] = -[K^{-1}]_\triangle$, and we obtain the same formulae (37). From (36) and (37), we obtain

$$\alpha_n \left(1 - (1 - \frac{k_\triangle}{k_\square})(I_T\omega \cdot t_\Gamma^\triangle)(x_\Gamma)\right) = (1 - \frac{k_\triangle}{k_\square})(I_T\rho \cdot t_\Gamma^\triangle)(x_\Gamma),$$

which yields the desired formula (35) for α_n, provided the denominator A does not vanish.

We next show that A indeed has a strictly positive lower bound, thanks to (28). If $k_\triangle \geq k_\square$, then using $1 - \frac{k_\triangle}{k_\square} \leq 0$ and $(I_T\omega \cdot t_\Gamma^\triangle)(x_\Gamma) \geq 0$, we obtain $A \geq 1$. If $k_\triangle < k_\square$, then we use $1 - \frac{k_\triangle}{k_\square} > 0$ and $(I_T\omega \cdot t_\Gamma^\triangle)(x_\Gamma) \leq 1$ to obtain $A \geq 1 - \left(1 - \frac{k_\triangle}{k_\square}\right) = \frac{k_\triangle}{k_\square}$.

Finally, let us focus on the coefficient β_t. Similarly to (36), we now impose that

$$1 = [K^{-1}\Lambda_t \cdot t_\Gamma](x_\Gamma) = \beta_t [K^{-1}\phi_t \cdot t_\Gamma](x_\Gamma),$$

which, thanks to the first equality of (37), translates into $\beta_t A = k_\triangle$, and thus yields the announced result. $\square$

5.3. Bounds of the specific shape functions

It is useful to bound the L^2-norm of Λ_n and Λ_t to subsequently bound the *a posteriori* error estimator η_T.

Lemma 5.5. *We have*

$$\|\Lambda_n\|_T \lesssim \frac{k_{\max}}{k_{\min}} \sum_{j=2}^{3} |F_j^\triangle|, \quad \|\Lambda_t\|_T \lesssim k_{\max} \sum_{j=2}^{3} |F_j^\triangle|.$$

Proof. From Lemma 5.4, we have, on the one hand,

$$\|\Lambda_n\|_T \leq |\alpha_n| \|\phi_t\|_T + \|\phi_n\|_T, \quad \|\Lambda_t\|_T \leq |\beta_t| \|\phi_t\|_T. \tag{38}$$

On the other hand, we have also shown in the proof of Lemma 5.4 that $A \geq \min\left\{1, \frac{k_\triangle}{k_\square}\right\}$, which allows us to bound α_n and β_t in the sequel from their expressions given in (35). If $k_{\max} = k_\triangle$, then using (29) and $A \geq 1$, we obtain

$$|\alpha_n| \lesssim \left|1 - \frac{k_{\max}}{k_{\min}}\right| \lesssim \frac{k_{\max}}{k_{\min}}, \quad 0 < \beta_t \leq k_{\max}, \tag{39}$$

whereas if $k_{\max} = k_\square$, we obtain, using again (29) and $A \geq \frac{k_\triangle}{k_\square}$, the same bound as above. In conclusion, α_n and β_t satisfy (39).

Thanks to Lemma 5.1 and (38), we can write

$$\|\Lambda_n\|_T \lesssim (|\alpha_n| + 1) \sum_{j=2}^{3} |F_j^\triangle|, \quad \|\Lambda_t\|_T \lesssim |\beta_t| \sum_{j=2}^{3} |F_j^\triangle|$$

which combined with (39) ends the proof. $\square$

Remark 4. In the case where the triangle $T \in \mathcal{T}_h^\Gamma$ is cut by one of its vertices into two sub-triangles, one may choose either of the two sub-triangles as T^Δ. The only changes in Section 5 occur in the sum $\sum_{j=2}^3 |F_j^\Delta|$, which is now replaced by the portion of the cut edge contained in ∂T^Δ, denoted $|F^\Delta|$.

6. Decomposition of the flux correction in the cut cells

In this section, we write $\sigma_h - K\nabla_h u_h$ on a cut cell T in terms of the shape functions Λ_n and Λ_t, in view of its further estimation in the next section.

First, we introduce $\varphi_0 \in \mathcal{RT}^0(T)$ uniquely defined by the conditions:

$$N_{T,j}(\varphi_0) = N_{T,j}(\sigma_h - K\nabla_h u_h) = \frac{1}{|F_j|}\int_{F_j} (\sigma_h - K\nabla_h u_h)\cdot n_T \,\mathrm{d}s, \quad 1 \le j \le 3. \tag{40}$$

Furthermore, since $\sigma_h \in \mathcal{IRT}^0(T)$ and $\mathrm{div}\varphi_0 \in P^0(T)$, one has

$$\mathrm{div}(\sigma_h - k_1\nabla u_{h,1} - \varphi_0)_{|T^1} = \mathrm{div}(\sigma_h - k_2\nabla u_{h,2} - \varphi_0)_{|T^2}.$$

Thus, $(\sigma_h - K\nabla_h u_h - \varphi_0) \in \mathcal{E}(T)$. Moreover, by definition of φ_0, one also has

$$\int_{F_j} (\sigma_h - K\nabla_h u_h - \varphi_0)\cdot n_T \,\mathrm{d}s = 0, \quad 1 \le j \le 3.$$

It follows that there exist $C_n, C_t \in \mathbb{R}$ such that $\mathcal{R}_T(\sigma_h - K\nabla_h u_h - \varphi_0) = (0,0,0,C_n,C_t)$. Since $\mathcal{R}_T$ is bijective according to Lemma 5.3, the previous relation combined with (32) yields the following decomposition on T:

$$\sigma_h - K\nabla_h u_h = \varphi_0 + C_n\Lambda_n + C_t\Lambda_t. \tag{41}$$

By writing

$$\begin{aligned}
[(\sigma_h - K\nabla_h u_h)\cdot n_\Gamma] &= [\varphi_0\cdot n_\Gamma] + C_n[\Lambda_n\cdot n_\Gamma] + C_t[\Lambda_t\cdot n_\Gamma],\\
[K^{-1}(\sigma_h - K\nabla_h u_h)\cdot t_\Gamma] &= [K^{-1}]\varphi_0\cdot t_\Gamma + C_n[K^{-1}\Lambda_n\cdot t_\Gamma] + C_t[K^{-1}\Lambda_t\cdot t_\Gamma]
\end{aligned}$$

and using the properties of φ_0, Λ_n, Λ_t, and σ_h, we can compute these constants as follows:

$$C_n = -[K\nabla_h u_h\cdot n_\Gamma], \quad C_t = -[K^{-1}]\varphi_0\cdot t_\Gamma(x_\Gamma) - [\nabla u_h\cdot t_\Gamma](x_\Gamma). \tag{42}$$

In the sequel, we are interested in bounding $\|\varphi_0\|_T$, $|C_n|$, and $|C_t|$. Clearly, from (26) we have

$$\|\varphi_0\|_T \le \sum_{j=1}^3 |N_{T,j}(\varphi_0)|\|\Lambda_{T,j}\|_T \lesssim h_T\sum_{j=1}^3 |N_{T,j}(\varphi_0)|. \tag{43}$$

Thanks to the definition of the flux σ_h, we obtain, for any edge $F_j \subset \partial T$,

$$(n_T\cdot n_{F_j})N_{T,j}(\varphi_0) = \frac{1}{|F_j|}\left(-\frac{n_T\cdot n_{F_j}}{2}\int_{F_j} k_i[\![\partial_n u_{h,i}]\!]\,\mathrm{d}s - \int_{F_j} k_i\theta_{h,i}\,\mathrm{d}s\right) \quad \text{if } F_j \in \mathcal{F}_h^i\backslash\mathcal{F}_h^\Gamma, \tag{44}$$

$$(n_T\cdot n_{F_j})N_{T,j}(\varphi_0) = \frac{1}{|F_j|}\sum_{i=1}^2\left(-\frac{n_T\cdot n_{F_j}}{2}\int_{F_j^i} k_i[\![\partial_n u_{h,i}]\!]\,\mathrm{d}s - \int_{F_j} k_i\theta_{h,i}\,\mathrm{d}s\right) \quad \text{if } F_j \in \mathcal{F}_h^\Gamma. \tag{45}$$

Lemma 6.1. *The following bound holds true:*

$$h_T \sum_{j=1}^{3} |N_{T,j}(\varphi_0)| \lesssim \sum_{T' \in \Delta_T} \left(h_{T'} \|f\|_{T'} + h_{T'}^{1/2} \sum_{i=1}^{2} \|k_i [\![\partial_n u_{h,i}]\!]\|_{\partial T' \setminus \partial \Delta_T} \right) + \sum_{i=1}^{2} k_i^{1/2} j_{i,\Delta_T}(u_{h,i}, u_{h,i})^{1/2}$$
$$+ \sum_{T' \in \mathcal{T}_h^\Gamma \cap \Delta_T} \left(\frac{k_{\min}}{h_{T'}^{1/2}} \|[u_h]\|_{\Gamma_{T'}} + h_{T'}^{1/2} \|[K \nabla u_h \cdot n_\Gamma]\|_{\Gamma_{T'}} \right).$$

Proof. Let F_j be a cut edge of T. Thanks to (45), the Cauchy–Schwarz inequality, and $|F_j^i| \leq |F_j|$, we have

$$|N_{T,j}(\varphi_0)| \leq \sum_{i=1}^{2} \left(\frac{1}{2|F_j|^{1/2}} \|k_i [\![\partial_n u_{h,i}]\!]\|_{F_j} + \frac{k_i}{|F_j|^{1/2}} \|\theta_{h,i}\|_{F_j} \right).$$

On a non-cut edge $F_j \in \mathcal{F}_h^i$, we obtain from (44) a similar bound as follows:

$$|N_{T,j}(\varphi_0)| \leq \frac{1}{2|F_j|^{1/2}} \|k_i [\![\partial_n u_{h,i}]\!]\|_{F_j} + \frac{k_i}{|F_j|^{1/2}} \|\theta_{h,i}\|_{F_j}.$$

The previous estimates lead to

$$h_T \sum_{j=1}^{3} |N_{T,j}(\varphi_0)| \lesssim \sum_{i=1}^{2} (h_T^{1/2} \|k_i [\![\partial_n u_{h,i}]\!]\|_{\partial T} + k_i h_T^{1/2} \|\theta_{h,i}\|_{\partial T}).$$

Next, the relation $(\theta_{h,i})_{|F} = (\theta_N^i)_{|F} + (\theta_M^i)_{|F}$ on any edge F of vertices N, M, together with the bound of the local multiplier θ_N^i given in Lemma 2.1, yields

$$\sum_{i=1}^{2} k_i h_T^{1/2} \|\theta_{h,i}\|_{\partial T} \lesssim \sum_{T' \in \Delta_T} \left(h_{T'} \|f\|_{T'} + \sqrt{h_{T'}} \sum_{i=1}^{2} \|k_i [\![\partial_n u_{h,i}]\!]\|_{\partial T' \setminus \partial \Delta_T} \right) + \sum_{i=1}^{2} k_i^{1/2} j_{i,\Delta_T}(u_{h,i}, u_{h,i})^{1/2}$$
$$+ \sum_{T' \in \mathcal{T}_h^\Gamma \cap \Delta_T} \left(\frac{k_\Gamma}{\sqrt{h_{T'}}} \|[u_h]\|_{\Gamma_{T'}} + \sqrt{h_{T'}} \|[K \nabla u_h \cdot n_\Gamma]\|_{\Gamma_{T'}} \right).$$

Combining the two previous estimates, we obtain the announced result. $\square$

Lemma 6.2. *We have*

$$|C_n| = \frac{1}{|\Gamma_T|^{1/2}} \|[K \nabla u_h \cdot n_\Gamma]\|_{\Gamma_T}, \quad |C_t| \lesssim |[K^{-1}]| \sum_{j=1}^{3} |N_{T,j}(\varphi_0)| + \frac{1}{|\Gamma_T|^{3/2}} \|[u_h]\|_{\Gamma_T}.$$

Proof. The first equality is obvious; it follows from (42) using that $[K \nabla u_h \cdot n_\Gamma]$ is constant on Γ_T. From the definition (42) of C_t, we obtain

$$|C_t| \leq |[K^{-1}]| |\varphi_0(x_\Gamma) \cdot t_\Gamma| + |[\nabla u_h \cdot t_\Gamma](x_\Gamma)|. \tag{46}$$

On the one hand, we have, thanks to (26),

$$|\varphi_0(x_\Gamma) \cdot t_\Gamma| \leq \sum_{j=1}^{3} |N_{T,j}(\varphi_0)| |\Lambda_{T,j}(x_\Gamma) \cdot t_\Gamma| \lesssim \sum_{i=1}^{3} |N_{T,j}(\varphi_0)|. \tag{47}$$

On the other hand, by means of an inverse inequality, we obtain

$$|[\nabla u_h \cdot t_\Gamma](x_\Gamma)|^2 = \frac{1}{|\Gamma_T|} \int_{\Gamma_T} [\nabla u_h \cdot t_\Gamma]^2 \, \mathrm{d}s \lesssim \frac{1}{|\Gamma_T|^3} \int_{\Gamma_T} [u_h]^2 \, \mathrm{d}s. \tag{48}$$

We obtain the announced estimate for C_t by using (47) and (48) in (46). □

7. Efficiency

In this section, we prove the local efficiency of each indicator η_T, $\tilde{\eta}_T$, and η_F, with respect to the following norm of the error:

$$\|v_h\|^2_{h,\Delta_T} = \sum_{i=1}^{2} \left(k_i \|\nabla v_{h,i}\|^2_{\Delta_T \cap \Omega^i} + j_{i,\Delta_T}(v_{h,i}, v_{h,i})\right) + \sum_{T \in \mathcal{T}_h^\Gamma \cap \Delta_T} \int_{\Gamma_T} \frac{k_\Gamma}{h_T} [v_h]^2 \, \mathrm{d}s.$$

The main difficulty lies in the treatment of the cut elements, in particular with regard to the dependence of the constants on the coefficients and on the mesh/interface geometry.

We begin with η_T and we bound it by the local error, with a constant C_T independent of the mesh, but dependent on the coefficients and the interface geometry and given explicitly. The proof for a cut triangle T uses the results of Sections 5 and 6 and is quite technical; therefore, we present it in several steps.

7.1. Bound of η_T by the residuals

The first step consists of bounding the local estimator η_T by a residual-type estimator, for any $T \in \mathcal{T}_h$.

Lemma 7.1. *If $T \in \mathcal{T}_h^i \backslash \mathcal{T}_h^\Gamma$ $(i = 1, 2)$, we have*

$$\eta_T \lesssim \sum_{T' \in \Delta_T} \left(\frac{h_{T'}}{k_i^{1/2}} \|f\|_{T'} + h_{T'}^{1/2} k_i^{1/2} (\|[\![\partial_n u_{h,i}]\!]\|_{\partial T' \backslash \partial \Delta_T} + \|[\![\partial_n u_{h,i}]\!]\|_{\partial T' \cap \mathcal{F}_g^i}) \right), \tag{49}$$

whereas if $T \in \mathcal{T}_h^\Gamma$, then

$$\begin{aligned} \eta_T \lesssim{}& \frac{k_{\max}}{k_{\min}} \sum_{T' \in \Delta_T} \left(\frac{h_{T'}}{k_{\min}^{1/2}} \|f\|_{T'} + \frac{h_{T'}^{1/2}}{k_{\min}^{1/2}} \sum_{i=1}^{2} \|k_i [\![\partial_n u_{h,i}]\!]\|_{\partial T' \backslash \partial \Delta_T} \right) + \frac{k_{\max}^{3/2}}{k_{\min}^{3/2}} \sum_{i=1}^{2} j_{i,\Delta_T}(u_{h,i}, u_{h,i})^{1/2} \\ &+ \frac{k_{\max}}{k_{\min}} \sum_{T' \in \mathcal{T}_h^\Gamma \cap \Delta_T} \left(\frac{k_{\min}^{1/2}}{|\Gamma_{T'}|^{1/2}} \|[u_h]\|_{\Gamma_{T'}} + \frac{h_{T'}^{1/2}}{k_{\min}^{1/2}} \|[K \nabla u_h \cdot n]\|_{\Gamma_{T'}} \right). \end{aligned} \tag{50}$$

Proof. The proof for a non-cut triangle is similar to the one given in Lemma 6.2 of [8], since $\sigma_h - k_i \nabla u_{h,i} \in \mathcal{RT}^0(T)$. In our setting, the Dirichlet condition on $\partial\Omega$ is imposed strongly, the diffusion coefficient is constant on each Ω^i, and we use linear finite elements, which simplifies the estimate of η_T given in [8]. In comparison to [8], we have an additional term on $\mathcal{F}_g^i$ in the right-hand side of (49). This term arises from the bound of $\theta_{h,i}$ given in Lemma 2.1 and accounts for the ghost penalization, which was not present in [8].

So in the sequel, we only treat the case $T \in \mathcal{T}_h^\Gamma$. We have, thanks to (41) and to the triangle inequality,

$$\|\sigma_h - K \nabla_h u_h\|_T \le \|\varphi_0\|_T + |C_n| \|\Lambda_n\|_T + |C_t| \|\Lambda_t\|_T.$$

From (43) and Lemmas 5.5 and 6.2, we obtain the following bound:

$$\|\sigma_h - K\nabla_h u_h\|_T \lesssim h_T \sum_{j=1}^{3} |N_{T,j}(\varphi_0)| + \frac{k_{\max}}{k_{\min}} \left(\sum_{j=2}^{3} |F_j^{\triangle}|\right) |\Gamma_T|^{-1/2} \|[K\nabla u_h \cdot n_\Gamma]\|_{\Gamma_T}$$
$$+ k_{\max} \left(\sum_{j=2}^{3} |F_j^{\triangle}|\right) \left(|[K^{-1}]| \sum_{j=1}^{3} |N_{T,j}(\varphi_0)| + |\Gamma_T|^{-3/2} \|[u_h]\|_{\Gamma_T} \right).$$

Using $k_{\max}|[K^{-1}]| = \frac{k_{\max}}{k_{\min}} - 1$ and $|F_j^{\triangle}| \le h_T$, we next obtain

$$\|\sigma_h - K\nabla_h u_h\|_T \lesssim \frac{k_{\max}}{k_{\min}} \left(h_T \sum_{j=1}^{3} |N_{T,j}(\varphi_0)| + \left(\sum_{j=2}^{3} |F_j^{\triangle}|\right) |\Gamma_T|^{-1/2} \|[K\nabla u_h \cdot n_\Gamma]\|_{\Gamma_T} \right.$$
$$\left. + k_{\min} \left(\sum_{j=2}^{3} |F_j^{\triangle}|\right) |\Gamma_T|^{-3/2} \|[u_h]\|_{\Gamma_T} \right).$$

Note that $\sum_{j=2}^{3} |F_j^{\triangle}| \lesssim |\Gamma_T|$, even in the worst cut case where $|\Gamma_T|$ is small, since then $\sum_{j=2}^{3} |F_j^{\triangle}|$ is of the same size as $|\Gamma_T|$. Using in addition $|F_j^{\triangle}| \le h_T$ and $|\Gamma_T| \le h_T$, we further obtain

$$\eta_T \le \frac{1}{k_{\min}^{1/2}} \|\sigma_h - K\nabla_h u_h\|_T \lesssim \frac{k_{\max}}{k_{\min}} \left(\frac{h_T}{k_{\min}^{1/2}} \sum_{j=1}^{3} |N_{T,j}(\varphi_0)| + \frac{h_T^{1/2}}{k_{\min}^{1/2}} \|[K\nabla u_h \cdot n_\Gamma]\|_{\Gamma_T} + \frac{k_{\min}^{1/2}}{|\Gamma_T|^{1/2}} \|[u_h]\|_{\Gamma_T} \right).$$

We next apply Lemma 6.1; by using $h_T^{-1/2} \le |\Gamma_T|^{-1/2}$ in front of $[u_h]$, we obtain (50) which ends the proof. □

Remark 5. The proof of Lemma 7.1 remains valid if $T \in \mathcal{T}_h^\Gamma$ is cut by one of its vertices into two sub-triangles. In this case, $\sum_{j=2}^{3} |F_j^{\Delta}|$ is replaced by $|F^{\Delta}|$, where F^{Δ} is the portion of the cut edge contained in ∂T^{Δ} (cf. Remark 4) and we still have $|F^{\Delta}| \lesssim |\Gamma_T|$.

7.2. Bound of the residuals by the local error

The second step consists of bounding the residual terms on the right-hand side of (49) and (50) by the error for any $T \in \mathcal{T}_h$. First, let us note that, thanks to the triangle inequality

$$\|f\|_T \le \|f_h\|_T + \|f - f_h\|_T,$$

it is sufficient to bound $\|f_h\|_T$ instead of $\|f\|_T$, the last term being contained in $\epsilon(T)$. The definitions of f_h and $\epsilon(T)$ can be found in Section 3.

We begin by treating the jump of the normal trace across an edge F of $T' \in \Delta_T$.

Lemma 7.2. *For $T \in \mathcal{T}_h^i \backslash \mathcal{T}_h^\Gamma$ $(1 \le i \le 2)$, one has*

$$\eta_T \lesssim |u - u_{h,i}|_{1,K,\Delta_T} + j_{i,\Delta_T}(u_{h,i}, u_{h,i})^{1/2} + \epsilon(\Delta_T) + \sum_{T' \in \Delta_T} \frac{h_{T'}}{k_i^{1/2}} \|f_h\|_{T'}, \tag{51}$$

whereas for $T \in \mathcal{T}_h^\Gamma$, one has

$$\eta_T \lesssim \frac{k_{\max}^{3/2}}{k_{\min}^{3/2}} (|u - u_h|_{1,K,\Delta_T} + \sum_{i=1}^{2} j_{i,\Delta_T}(u_{h,i}, u_{h,i})^{1/2}) + \frac{k_{\max}}{k_{\min}^{3/2}} \sum_{T' \in \Delta_T} h_{T'} \|f_h\|_{T'}$$

$$+\frac{k_{\max}}{k_{\min}}\sum_{T'\in\mathcal{T}_h^\Gamma\cap\Delta_T}\left(\frac{k_{\min}^{1/2}}{|\Gamma_{T'}|^{1/2}}\|[u_h]\|_{\Gamma_{T'}}+\frac{h_{T'}^{1/2}}{k_{\min}^{1/2}}\|[K\nabla u_h\cdot n]\|_{\Gamma_{T'}}\right)+\frac{k_{\max}^{3/2}}{k_{\min}^{3/2}}\epsilon(\Delta_T). \tag{52}$$

Proof. Assume first $T\in\mathcal{T}_h^i\backslash\mathcal{T}_h^\Gamma$. Let $T'\in\Delta_T$ and $F\subset\partial T'$. Thanks to the shape regularity of the triangle T', we have $h_{T'}\lesssim h_F$. If $F\in\mathcal{F}_g^i$, then the term $h_{T'}^{1/2}k_i^{1/2}\|[\![\partial_n u_{h,i}]\!]\|_F$ is easily bounded by the ghost-penalty term $j_i(u_{h,i},u_{h,i})^{1/2}$ restricted to F. Otherwise, we have $T_F^+\cup T_F^-\subset\Omega^i$ and the well-known Verfürth argument (see, for instance, Proposition 4.2. of [21]) yields

$$h_{T'}^{1/2}k_i^{1/2}\|[\![\partial_n u_{h,i}]\!]\|_F\lesssim|u-u_{h,i}|_{1,K,T_F^+\cup T_F^-}+\epsilon(T_F^+\cup T_F^-).$$

By abuse of notation, we denote in the same way the set of triangles Δ_T and the domain they cover. For $F\subset\partial T'\backslash\partial\Delta_T$, we also have $T_F^+\cup T_F^-\subset\Delta_T$; therefore, (51) follows from (49).

Assume now $T\in\mathcal{T}_h^\Gamma$ and let again $T'\in\Delta_T$. For $F\subset\partial T'\backslash\partial\Delta_T$, we bound, for $i=1,2$, the term $h_{T'}^{1/2}k_i^{1/2}\|[\![\partial_n u_{h,i}]\!]\|_F$ as previously, by means of Verfürth' argument. Using furthermore that $\|k_i[\![\partial_n u_{h,i}]\!]\|_F\leq k_{\max}^{1/2}k_i^{1/2}\|[\![\partial_n u_{h,i}]\!]\|_F$, we finally obtain (52) from (50). $\square$

Next, we focus on the term containing the data f_h.

Lemma 7.3. *If $T\in\mathcal{T}_h^i\backslash\mathcal{T}_h^\Gamma$, then*

$$h_T\|f_h\|_T\lesssim\|k_i\nabla(u-u_{h,i})\|_T+h_T\|f-f_h\|_T,$$

whereas if $T\in\mathcal{T}_h^\Gamma$, one has

$$h_T\|f_h\|_T\lesssim\sum_{i=1}^2\|k_i\nabla(u-u_{h,i})\|_{T^i}+h_T^{1/2}\|[K\nabla u_h\cdot n_\Gamma]\|_{\Gamma_T}+h_T\|f-f_h\|_T.$$

Proof. We only treat below the case of a cut triangle, the other one being standard. Following Verfürth's argument (cf. [21]), we let $b_T=27\lambda_1\lambda_2\lambda_3$ be the cubic bubble function on T and consider $w_T=f_hb_T$, which satisfies

$$\|f_h\|_T^2\lesssim\int_T f_hw_T\,\mathrm{d}x,\quad\|\nabla w_T\|_T\lesssim h_T^{-1}\|w_T\|_T\lesssim h_T^{-1}\|f_h\|_T. \tag{53}$$

We start with

$$\|f_h\|_T^2\lesssim\int_T fw_T\,\mathrm{d}x+\int_T(f_h-f)w_T\,\mathrm{d}x\lesssim\int_T fw_T\,\mathrm{d}x+\|f-f_h\|_T\|f_h\|_T.$$

Since $k_i\nabla u_{h,i}$ is piecewise constant on Ω_h^i for $i=1,2$, it follows that $\operatorname{div}(k_i\nabla u_{h,i})_{|T^i}=0$. Using also $w_{T|\partial T}=0$, we obtain, by integrating by parts on each $T^i=T\cap\Omega^i$,

$$\begin{aligned}\int_T fw_T\,\mathrm{d}x&=-\sum_{i=1}^2\int_{T^i}\operatorname{div}(k_i\nabla(u-u_{h,i}))w_T\,\mathrm{d}x\\&=\sum_{i=1}^2\int_{T^i}k_i\nabla(u-u_{h,i})\cdot\nabla w_T\,\mathrm{d}x-\int_{\Gamma_T}[K\nabla(u-u_h)\cdot n_\Gamma]w_T\,\mathrm{d}s\\&\lesssim\|\nabla w_T\|_T\left(\sum_{i=1}^2\|k_i\nabla(u-u_{h,i})\|_{T^i}\right)+\|w_T\|_{\Gamma_T}\|[K\nabla(u-u_h)\cdot n_\Gamma]\|_{\Gamma_T}.\end{aligned}$$

From the trace inequality (3) and the properties (53) of w_T, it follows that

$$\|w_T\|_{\Gamma_T} \lesssim \frac{1}{h_T^{1/2}}\|w_T\|_T + h_T^{1/2}\|\nabla w_T\|_T \lesssim h_T^{-1/2}\|f_h\|_T,$$

which finally implies, thanks to $[K\nabla u \cdot n_\Gamma] = 0$, that

$$\|f_h\|_T \lesssim h_T^{-1}\sum_{i=1}^{2}\|k_i\nabla(u-u_{h,i})\|_{T^i} + h_T^{-1/2}\|[K\nabla u_h \cdot n_\Gamma]\|_{\Gamma_T} + \|f-f_h\|_T.$$

Multiplying the previous inequality by h_T yields the announced result. $\square$

Finally, we are interested in bounding the term $\|[K\nabla u_h \cdot n_\Gamma]\|_{\Gamma_T}$. For theoretical reasons only, to obtain the best constant, we make the following assumption.

Assumption 1. *For any $T \in \mathcal{T}_h^\Gamma$, there exist closed, regular-shaped triangles $\tilde{T}^1 \subset \Omega^1, \tilde{T}^2 \subset \Omega^2$ such that they have Γ_T as a common side: $\tilde{T}^1 \cap \tilde{T}^2 = \Gamma_T$.*

Since $|\Gamma_T| \le h_T$, we can moreover suppose, without loss of generality, that $\tilde{T}^i$ are included in the neighborhood of T consisting of the triangles sharing an edge with T.

Remark 6. The particular situation where Assumption 1 might not hold is discussed in [15], p. 156. It leads to a similar estimate, with an efficiency constant multiplied by $k_{\max}^{1/2}/k_{\min}^{1/2}$. However, we have not noticed any influence of Assumption 1 in the numerical experiments, see [9].

Lemma 7.4. *Under Assumption 1, we have for any $T \in \mathcal{T}_h^\Gamma$:*

$$h_T^{1/2}\|[K\nabla u_h \cdot n_\Gamma]\|_{\Gamma_T} \lesssim \sum_{i=1}^{2}\left(\frac{h_T^{1/2}k_i^{1/2}}{|\Gamma_T|^{1/2}}\|k_i^{1/2}\nabla(u_{h,i}-u)\|_{\tilde{T}^i} + h_T\|f-f_h\|_{\tilde{T}^i}\right) + \sum_{i=1}^{2}k_i^{1/2}j_{i,\Delta_T}(u_{h,i},u_{h,i})^{1/2}.$$

Proof. We use a similar argument to [17] for the immersed finite element method, that is, we consider the bubble function b_Γ on Γ_T, which takes the value 1 at the midpoint of Γ_T and satisfies $(b_\Gamma)_{|\partial(\tilde{T}^1\cup\tilde{T}^2)} = 0$ and $(b_\Gamma)_{|\tilde{T}^i} \in P^2(\tilde{T}^i)$ for $i = 1, 2$. It is useful to note that for any regular-shaped triangle $T^* \in \{\tilde{T}^1, \tilde{T}^2\}$, we have

$$\|\nabla b_\Gamma\|_{T^*} \lesssim \frac{1}{|\Gamma_T|}\|b_\Gamma\|_{T^*} \lesssim 1.$$

Let then $\psi_\Gamma = [K\nabla u_h \cdot n_\Gamma]b_\Gamma$, which satisfies, for $T^* \in \{\tilde{T}^1, \tilde{T}^2\}$,

$$\|\nabla\psi_\Gamma\|_{T^*} \lesssim \frac{1}{|\Gamma_T|}\|\psi_\Gamma\|_{T^*} \lesssim \frac{1}{|\Gamma_T|^{1/2}}\|[K\nabla u_h \cdot n_\Gamma]\|_{\Gamma_T}, \tag{54}$$

$$\|[K\nabla u_h \cdot n_\Gamma]\|_{\Gamma_T}^2 \lesssim \left|\int_{\Gamma_T}[K\nabla u_h \cdot n_\Gamma]\psi_\Gamma \,\mathrm{d}s\right|. \tag{55}$$

Using the continuity of $K\nabla u \cdot n_\Gamma$ across Γ and integrating by parts on each $\tilde{T}^i$, we obtain, since $(\psi_\Gamma)_{|(\partial\tilde{T}^i\setminus\Gamma_T)} = 0$,

$$\int_{\Gamma_T}[K\nabla u_h \cdot n_\Gamma]\psi_\Gamma \,\mathrm{d}s = \sum_{i=1}^{2}\left(\int_{\tilde{T}^i}k_i\nabla(u_{h,i}-u)\cdot\nabla\psi_\Gamma \,\mathrm{d}x + \int_{\tilde{T}^i}f\psi_\Gamma \,\mathrm{d}x - \sum_{F^*\in\mathcal{F}(\tilde{T}^i)}\int_{F^*}k_i[\![\partial_n(u_{h,i}-u)]\!]\psi_\Gamma \,\mathrm{d}s\right),$$

where the set $\mathcal{F}(\tilde{T}^i)$ contains the possible intersections of the sides of $\mathcal{F}_h^i$ with $\tilde{T}^i$. Using next the Cauchy–Schwarz inequality, we obtain

$$\left| \int_{\Gamma_T} [K\nabla u_h \cdot n_\Gamma]\psi_\Gamma \,\mathrm{d}s \right| \leq \sum_{i=1}^{2} (\|k_i \nabla(u_{h,i} - u)\|_{\tilde{T}^i} \|\nabla\psi_\Gamma\|_{\tilde{T}^i} + \|f\|_{\tilde{T}^i} \|\psi_\Gamma\|_{\tilde{T}^i}) + \sum_{i=1}^{2} \sum_{F^* \in \mathcal{F}(\tilde{T}^i)} \|k_i [\![\partial_n u_{h,i}]\!]\|_{F^*} \|\psi_\Gamma\|_{F^*}. \tag{56}$$

Let $F^* \in \mathcal{F}(\tilde{T}^i)$. We next apply the trace inequality (3) to the discrete function ψ_Γ on the triangle $\tilde{T}^i$ cut by F^*; using also an inverse inequality and the fact that $\tilde{T}^i$ is a regular triangle of size $|\Gamma_T|$, we obtain $\|\psi_\Gamma\|_{F^*} \lesssim |\Gamma_T|^{-1/2} \|\psi_\Gamma\|_{\tilde{T}^i}$. Together with the properties (54) and (55) of ψ_Γ, inequality (56) yields

$$\|[K\nabla u_h \cdot n_\Gamma]\|_{\Gamma_T} \lesssim \sum_{i=1}^{2} \left(\frac{k_i^{1/2}}{|\Gamma_T|^{1/2}} \|k_i^{1/2} \nabla(u_{h,i} - u)\|_{\tilde{T}^i} + |\Gamma_T|^{1/2} \|f\|_{\tilde{T}^i} + \sum_{F^* \in \mathcal{F}(\tilde{T}^i)} \|k_i [\![\partial_n u_{h,i}]\!]\|_{F^*} \right). \tag{57}$$

Thanks to Verfürth's argument with the cubic bubble function on the triangle $\tilde{T}^i$ (of size $|\Gamma_T|$), we have, as in Lemma 7.3, the following estimate:

$$\|f_h\|_{\tilde{T}^i} \lesssim \frac{1}{|\Gamma_T|} \|k_i \nabla(u_{h,i} - u)\|_{\tilde{T}^i} + \frac{1}{|\Gamma_T|^{1/2}} \sum_{F^* \in \mathcal{F}(\tilde{T}^i)} \|k_i [\![\partial_n u_{h,i}]\!]\|_{F^*} + \|f - f_h\|_{\tilde{T}^i}, \quad i = 1, 2.$$

Using also the triangle inequality and $|\Gamma_T| \leq h_T$, we finally obtain, for $i = 1, 2$,

$$|\Gamma_T|^{1/2} \|f\|_{\tilde{T}^i} \lesssim \frac{k_i^{1/2}}{|\Gamma_T|^{1/2}} \|k_i^{1/2} \nabla(u_{h,i} - u)\|_{\tilde{T}^i} + \sum_{F^* \in \mathcal{F}(\tilde{T}^i)} \|k_i [\![\partial_n u_{h,i}]\!]\|_{F^*} + h_T^{1/2} \|f - f_h\|_{\tilde{T}^i}. \tag{58}$$

In addition, we note that for $i = 1, 2$, any $F^* \in \mathcal{F}_h(\tilde{T}^i)$ is included in a side of $\mathcal{F}_g^i \cap \mathcal{F}_{T'}$ for a triangle $T' \in \Delta_T$. Together with $h_T \lesssim h_F$, this gives

$$\sum_{F^* \in \mathcal{F}(\tilde{T}^i)} \|k_i [\![\partial_n u_{h,i}]\!]\|_{F^*} \lesssim \sum_{T' \in \Delta_T} \sum_{F \in \mathcal{F}_g^i \cap \mathcal{F}_{T'}} \|k_i [\![\partial_n u_{h,i}]\!]\|_F \lesssim \frac{k_i^{1/2}}{h_T^{1/2}} j_{i,\Delta_T}(u_{h,i}, u_{h,i})^{1/2}. \tag{59}$$

We conclude using (58) and (59) in (57) and multiplying by $h_T^{1/2}$. $\square$

7.3. Final bound of η_T

We now give the main result of this section, which ascertains the local efficiency of the error estimator η_T.

Theorem 7.5. *Under Assumption 1, for any $T \in \mathcal{T}_h$ there exists a positive constant C_T such that*

$$\forall T \in \mathcal{T}_h, \quad \eta_T \lesssim C_T \left(\|u - u_h\|_{h,\Delta_T} + \epsilon(\Delta_T) \right),$$

with $C_T = 1$ if $T \in \mathcal{T}_h \backslash \mathcal{T}_h^\Gamma$ and $C_T = \max_{T' \in \Delta_T \cap \mathcal{T}_h^\Gamma} \frac{h_{T'}^{1/2}}{|\Gamma_{T'}|^{1/2}} \frac{k_{\max}^{3/2}}{k_{\min}^{3/2}}$ if $T \in \mathcal{T}_h^\Gamma$.

Proof. It is sufficient to gather the results that we have proved so far in order to bound η_T. The estimate for a non-cut triangle is obvious; it follows from (51) combined with the first estimate of Lemma 7.3. Therefore, we assume next that $T \in \mathcal{T}_h^\Gamma$.

Thanks to Lemma 7.4, we can improve the second estimate of Lemma 7.3:

$$\frac{h_T}{k_{\min}^{1/2}}\|f_h\|_T \lesssim \frac{h_T}{k_{\min}^{1/2}}(\|f-f_h\|_T + \|f-f_h\|_{\tilde{T}^1\cup\tilde{T}^2}) + \frac{k_{\max}^{1/2}}{k_{\min}^{1/2}}\sum_{i=1}^{2}\left(|u-u_{h,i}|_{1,K,T^i} + \frac{h_T^{1/2}}{|\Gamma_T|^{1/2}}|u-u_{h,i}|_{1,K,\tilde{T}^i} + j_{i,\Delta_T}(u_{h,i},u_{h,i})^{1/2}\right).$$

We use this estimate on any cut triangle $T' \in \mathcal{T}_h^\Gamma \cap \Delta_T$, as well as Lemma 7.4 in inequality (52). With $h_{T'} \geq |\Gamma_{T'}|$, we finally obtain

$$\eta_T \lesssim \frac{k_{\max}^{3/2}}{k_{\min}^{3/2}}\left(\max_{T'\in\Delta_T\cap\mathcal{T}_h^\Gamma}\frac{h_{T'}^{1/2}}{|\Gamma_{T'}|^{1/2}}|u-u_h|_{1,K,\Delta_T} + \sum_{i=1}^{2} j_{i,\Delta_T}(u_{h,i},u_{h,i})^{1/2} + \epsilon(\Delta_T)\right) + \frac{k_{\max}}{k_{\min}}\sum_{T'\in\mathcal{T}_h^\Gamma\cap\Delta_T}\frac{h_{T'}^{1/2}}{|\Gamma_{T'}|^{1/2}}\frac{k_\Gamma^{1/2}}{h_{T'}^{1/2}}\|[u_h]\|_{\Gamma_{T'}} \lesssim C_T\|u-u_h\|_{h,\Delta_T} + \frac{k_{\max}^{3/2}}{k_{\min}^{3/2}}\epsilon(\Delta_T)$$

which concludes the proof. □

7.4. Bounds of $\tilde{\eta}_T$ and η_F

The bound of $\tilde{\eta}_T$ on any cut triangle $T \in \mathcal{T}_h^\Gamma$ is immediate, since $\tilde{\eta}_T$ already appears in the error $\|\cdot\|_{h,T}$, with a different scaling.

Theorem 7.6. *Let $T \in \mathcal{T}_h^\Gamma$. There exists a positive constant $\tilde{C}_T$ such that*

$$\tilde{\eta}_T \leq \tilde{C}_T\|u-u_h\|_{h,T}, \quad \textit{with} \quad \tilde{C}_T = \frac{h_T}{\sqrt{h_T^{\min}|\Gamma_T|}}.$$

Proof. By definition, we have

$$\tilde{\eta}_T = \frac{\sqrt{h_T k_\Gamma}}{\sqrt{h_T^{\min}|\Gamma_T|}}\|[u_h]\|_{\Gamma_T} = \frac{h_T}{\sqrt{h_T^{\min}|\Gamma_T|}}\frac{k_\Gamma^{1/2}}{h_T^{1/2}}\|[u_h]\|_{\Gamma_T} \leq \tilde{C}_T\|u-u_h\|_{h,T},$$

which is the desired estimate. □

It remains to bound the indicator η_F on a cut edge.

Theorem 7.7. *Let $F \in \mathcal{F}_h^\Gamma$. There exists a positive constant C_F such that*

$$\eta_F \lesssim C_F\left(\|u-u_h\|_{h,\Delta_F} + \epsilon(\Delta_F)\right) \quad \textit{with} \;\; C_F = \max_{T\in\Delta_F\cap\mathcal{T}_h^\Gamma}\frac{h_T}{|\Gamma_T|}\frac{k_{\max}^{3/2}}{k_{\min}^{3/2}}.$$

Proof. By the definition of η_F and the inequality $\|a+b\|^2 \leq 2(\|a\|^2+\|b\|^2)$, we have

$$\eta_F^2 = \frac{h_F}{k_\Gamma}\sum_{i=1}^{2}\int_{F^i}[\![(\sigma_h - k_i\nabla u_{h,i})\cdot n_F + k_i\nabla u_{h,i}\cdot n_F]\!]^2\,\mathrm{d}s$$
$$\leq \frac{2h_F}{k_\Gamma}\sum_{i=1}^{2}\left(\int_{F^i}[\![\sigma_h\cdot n_F - k_i\nabla u_{h,i}\cdot n_F]\!]^2\,\mathrm{d}s + \int_{F^i}k_i^2[\![\partial_n u_{h,i}]\!]^2\,\mathrm{d}s\right).$$

Using for the last integral that $F^i \subset F$, we obtain

$$\eta_F^2 \leq \frac{2h_F}{k_\Gamma}\|[\![(\sigma_h - K\nabla_h u_h)\cdot n_F]\!]\|_F^2 + \sum_{i=1}^{2}\frac{2k_i}{k_\Gamma} j_{i,\Delta_F}(u_{h,i}, u_{h,i}). \tag{60}$$

Since $k_i/k_\Gamma \lesssim k_{\max}/k_{\min} \leq C_F \leq C_F^2$, we only have to bound the first term on the right-hand side of (60) to establish the theorem.

Let $\{F\} = \partial T_F^+ \cap \partial T_F^-$. By the triangle inequality, it is sufficient to bound $\|(\sigma_h - K\nabla_h u_h)_{|T}\cdot n_F\|_F$ for any $T \in \{T_F^+, T_F^-\}$. Using the decomposition (41) of $\sigma_h - K\nabla_h u_h$ on T, we obtain

$$\|(\sigma_h - K\nabla_h u_h)_{|T}\cdot n_F\|_F \leq \|\varphi_0 \cdot n_F\|_F + |C_n|\|\Lambda_n \cdot n_F\|_F + |C_t|\|\Lambda_t \cdot n_F\|_F. \tag{61}$$

For $\varphi_0 \in \mathcal{RT}^0(T)$, it is known that

$$\sqrt{h_F}\|\varphi_0 \cdot n_F\|_F \lesssim \|\varphi_0\|_T \leq h_T \sum_{j=1}^{3}|N_{T,j}(\varphi_0)|, \tag{62}$$

whereas from the definition (34) of Λ_n and Λ_t, together with the property $(I_T w)\cdot n_F = \pi_F^0(w\cdot n_F)$, we obtain

$$\|\Lambda_n \cdot n_F\|_F \leq 2|\alpha_n|\|\omega\cdot n_F\|_F + 2\|\rho\cdot n_F\|_F, \quad \|\Lambda_t\cdot n_F\|_F \leq 2|\beta_t|\|\rho\cdot n_F\|_F.$$

Thanks to the definition (27) of ω and ρ, it follows, with $F^\triangle = F\cap \partial T^\triangle$, that:

$$\|\rho\cdot n_F\|_F^2 = \int_{F^\triangle} |\, n_\Gamma^\triangle \cdot n_F|^2 \,\mathrm{d}s \leq |F^\triangle|, \quad \|\omega\cdot n_F\|_F^2 = \int_{F^\triangle} |\, t_\Gamma^\triangle\cdot n_F|^2\,\mathrm{d}s \leq |F^\triangle|.$$

Using the bound (39) for the coefficients α_n and β_t and Lemma 6.2, we end up with

$$\begin{aligned}
|C_n|\|\Lambda_n\cdot n_F\|_F &\lesssim \frac{k_{\max}}{k_{\min}}\frac{|F^\triangle|^{1/2}}{|\Gamma_T|^{1/2}}\|[K\nabla u_h\cdot n_\Gamma]\|_{\Gamma_T},\\
|C_t|\|\Lambda_t\cdot n_F\|_F &\lesssim |F^\triangle|^{1/2}k_{\max}\left(|[K^{-1}]|\sum_{j=1}^{3}|N_{T,j}(\varphi_0)| + \frac{1}{|\Gamma_T|^{3/2}}\|[u_h]\|_{\Gamma_T}\right)\\
&\lesssim h_F^{1/2}\frac{k_{\max}}{k_{\min}}\sum_{j=1}^{3}|N_{T,j}(\varphi_0)| + k_{\max}\frac{|F^\triangle|^{1/2}}{|\Gamma_T|^{3/2}}\|[u_h]\|_{\Gamma_T}.
\end{aligned}$$

Using the previous bounds and (62) in (61), as well as $|F^\triangle| \lesssim |\Gamma_T|$, we obtain

$$\frac{\sqrt{h_F}}{\sqrt{k_\Gamma}}\|(\sigma_h - K\nabla_h u_h)_{|T}\cdot n_F\|_F \lesssim \frac{k_{\max}}{k_{\min}}\left(\frac{h_T}{\sqrt{k_\Gamma}}\sum_{j=1}^{3}|N_{T,j}(\varphi_0)| + \frac{\sqrt{h_F}}{\sqrt{k_\Gamma}}\|[K\nabla u_h\cdot n_\Gamma]\|_{\Gamma_T} + \frac{\sqrt{h_F k_\Gamma}}{|\Gamma_T|}\|[u_h]\|_{\Gamma_T}\right).$$

Thanks to Lemmas 6.1, 7.3 and 7.4, we finally deduce that

$$\frac{\sqrt{h_F}}{\sqrt{k_\Gamma}}\|(\sigma_h - K\nabla_h u_h)_{|T}\cdot n_F\|_F \lesssim \max_{T'\in\Delta_T\cap\mathcal{T}_h^\Gamma}\frac{h_{T'}}{|\Gamma_{T'}|}\frac{k_{\max}^{3/2}}{k_{\min}^{3/2}}\left(\|u-u_h\|_{h,\Delta_F} + \epsilon(\Delta_F)\right).$$

We conclude by summing upon $T \in \{T_F^+, T_F^-\}$ and by using (60). $\square$

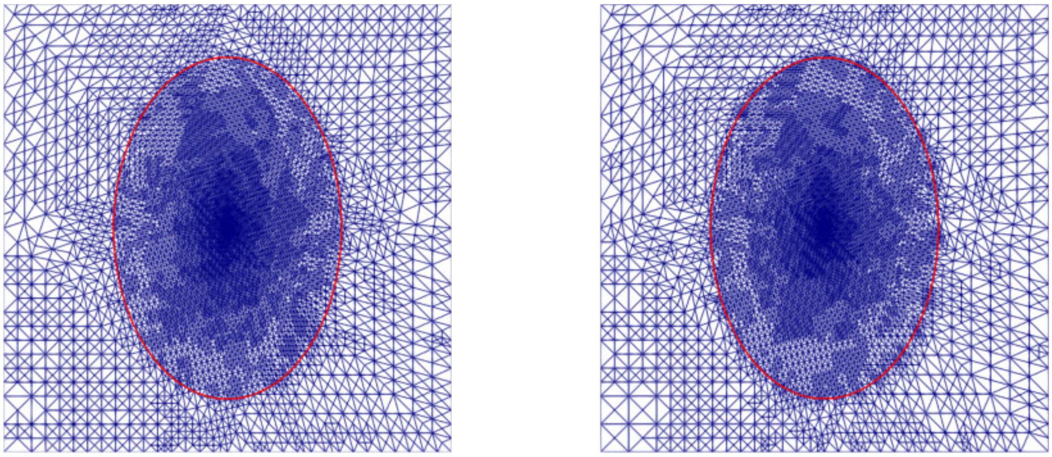

(a) Final mesh (iteration 14) using η_T (b) Final mesh (iteration 12) using $\bar{\eta}_T$

FIGURE 2. Example 8.1. Final adapted meshes for $\mu = 10$.

8. Numerical simulations

To illustrate the theoretical results, we present several numerical experiments. In [9], we validated both the flux implementation and the AMR strategy based on the error indicator η_T, which is easier to implement and computationally cheaper than $\bar{\eta}_T := \eta_T + \tilde{\eta}_T + \sum_{F\in\mathcal{F}_h^\Gamma\cap\partial T} \eta_F$. In the following, we investigate the numerical behavior of η, η_Γ, and the error under two AMR procedures, using either η_T or $\bar{\eta}_T$ as local error indicators, to justify the use of η_T in [9]. Moreover, we numerically show optimal convergence and robustness with respect to the diffusion contrast and to the mesh/interface configuration, even in situations where the theoretical constants may blow up. We consider three test cases.

Example 8.1 (Ellipse problem)**.** Let $\Omega = [-1,1]^2$ and let Γ be the ellipse centered at the origin, of equation $\rho = 1$ where $\rho = \sqrt{\frac{x^2}{a^2} + \frac{y^2}{b^2}}$, with $2a$ the width and $2b$ the height of the ellipse. The exact solution of (2) with $g = 0$ is given by

$$u(\rho) = \frac{1}{k_1}\sqrt{\rho} \quad \text{if } \rho \le 1, \quad u(\rho) = \frac{1}{k_2}\sqrt{\rho} + \frac{1}{k_1} - \frac{1}{k_2} \quad \text{if } \rho > 1.$$

Here, we take $a = \frac{\pi}{6.18}$, $b = 1.5a$, $k_1 = 1$ and let $k_2 = \mu k_1$. For $\mu \neq 1$, the solution is merely in $H^{\frac{3}{2}-\varepsilon}(\Omega)$ for any $\varepsilon > 0$ and becomes singular at the origin.

We are interested in testing the influence of the additional indicator η_Γ in the AMR procedure. We recall that η_Γ^2 is the sum of two contributions: $\sum_{F\in\mathcal{F}_h^\Gamma} \eta_F^2$, which we denote in the sequel by $\hat{\eta}$ and which is due to the definition of the immersed Raviart–Thomas space on the cut edges, and $\sum_{T\in\mathcal{T}_h^\Gamma} \tilde{\eta}_T^2$, which is inherent to the CutFEM formulation and which is due to the discontinuity of u_h across Γ.

The stopping AMR criterion is that the total number of degrees of freedom N is less than 25,000. We first take $\mu = 10$ and perform two AMR procedures, one based on the main error indicator η_T for any $T \in \mathcal{T}_h$, and the other on the indicator $\bar{\eta}_T = \eta_T + \tilde{\eta}_T + \sum_{F\in\mathcal{F}_h^\Gamma\cap\partial T} \eta_F$. Figure 2 shows the final meshes obtained with these refinement procedures. One can observe that they are very similar and that the refinement mainly focuses near the singularity, as expected.

We also compare the estimators η, $\eta + \hat{\eta}$, and $\eta + \eta_\Gamma$. Their decay rate over the last 10 refinement iterations is shown in Figure 3, while in Table 1 we report the values of η, $\eta + \eta_\Gamma$ and the effectivity index for the final

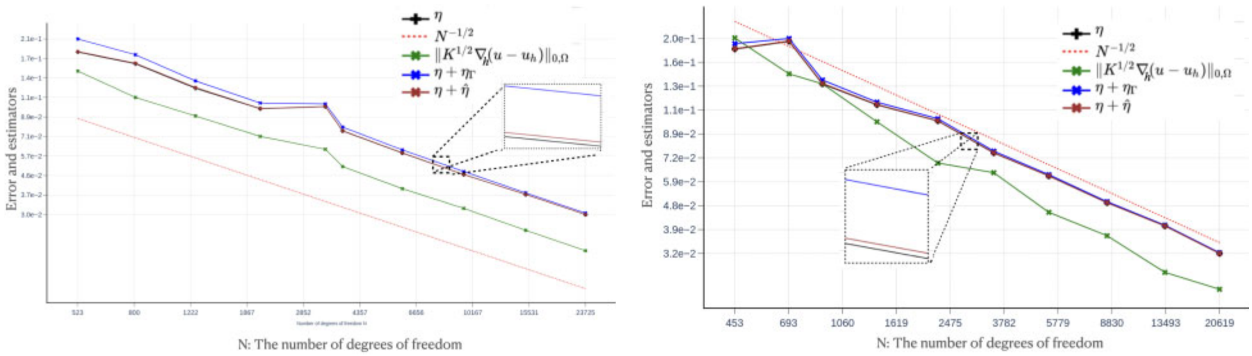

(a) AMR using η_T (b) AMR using $\bar{\eta}_T$

FIGURE 3. Example 8.1. Convergence rate of the error, η, $\eta + \hat{\eta}$ and $\eta + \eta_\Gamma$ for $\mu = 10$.

TABLE 1. Example 8.1. Estimators and effectivity index: last iterations for $\mu = 10$.

(a) AMR using only η_T				(b) AMR using $\bar{\eta}_T$			
N	$\eta + \eta_\Gamma$	η	η/err	N	$\eta + \eta_\Gamma$	η	$(\eta + \eta_\Gamma)/err$
3,830	7.9×10^{-2}	7.5×10^{-2}	1.48	3,486	7.6×10^{-2}	7.5×10^{-2}	1.20
5,995	6.1×10^{-2}	5.9×10^{-2}	1.4	5,379	6.2×10^{-2}	6.1×10^{-2}	1.38
9,511	4.8×10^{-2}	4.6×10^{-2}	1.45	8,506	4.9×10^{-2}	4.9×10^{-2}	1.34
15,142	3.8×10^{-2}	3.7×10^{-2}	1.49	13,410	4.0×10^{-2}	4.0×10^{-2}	1.50
23,725	3×10^{-2}	2.9×10^{-2}	1.49	20,619	3.1×10^{-2}	3.1×10^{-2}	1.37

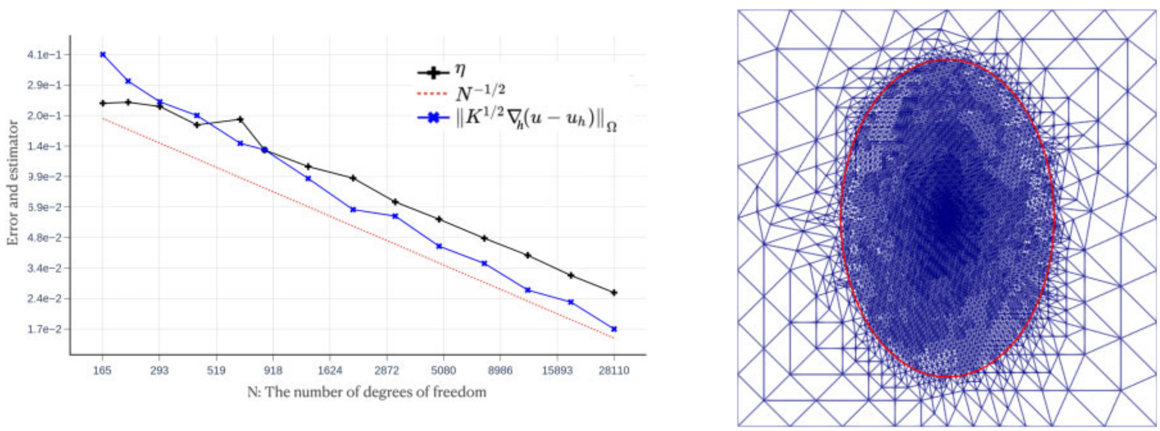

(a) Convergence rate for the exact error and η (b) Final mesh (iteration 13)

FIGURE 4. Example 8.1. AMR using η_T: estimator and error convergence (*left*) and final mesh (*right*) for $\mu = 10^6$.

iterations. One can see that the two AMR procedures yield similar results and moreover, that the additional estimator η_Γ is quite small. We conclude that η_Γ can be neglected in the AMR, which substantially simplifies the latter. The effectivity index, that is, the ratio between the employed global indicator and the H^1 semi-norm

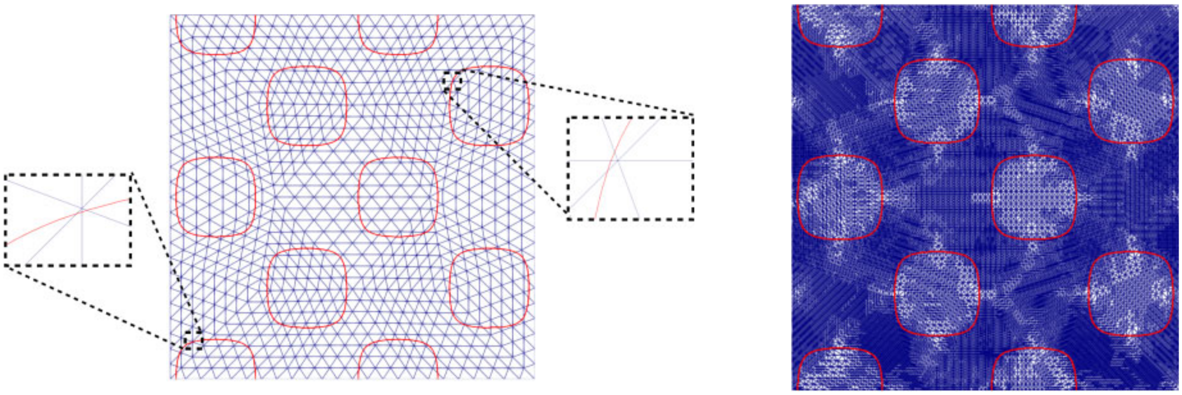

(a) Initial mesh (iteration 0) (b) Final mesh (iteration 13)

FIGURE 5. Example 8.2. Initial and final meshes.

of the error $err = \|K^{1/2}\nabla_h(u-u_h)\|_\Omega$, is slightly smaller when using the indicator $\tilde{\eta}_T$ in the AMR. This is in agreement with the theoretical results, since the reliability was established for $\eta+\eta_\Gamma$.

Finally, we consider a large jump in the diffusion coefficients, namely, $\mu = 10^6$. Figure 4 shows the convergence rate for both the error and the estimator η, as well as the final mesh obtained using only the indicator η_T for adaptive refinement. Although the ratio $k_{\max}/k_{\min}$ is large, and hence the (theoretical) efficiency constant C_T is large (independently of the mesh/interface cut), this does not seem to influence the estimator behavior, since we retrieve the optimal convergence rate $O(N^{-1/2})$.

Example 8.2 (Sinusoidal interface problem)**.** We next consider an interface problem in the square domain $\Omega = [-1,1]^2$, with several interfaces described by the periodic level set function $\phi(x,y) = \sin(2\pi x)\cos(2\pi y) - 0.2$. Thus, $\Gamma = \{(x,y) \in \Omega;\ \phi(x,y) = 0\}$. The diffusion coefficient is as follows:

$$k(x,y) = 1 \quad \text{if } \phi(x,y) < 0, \qquad k(x,y) = 100 \quad \text{if } \phi(x,y) \geq 0.$$

The exact solution is given by $u(x,y) = \dfrac{1}{k(x,y)}\phi(x,y)$ for $(x,y) \in \Omega$.

In this example, we use only η_T as error indicator in AMR. The stopping criterion is that $N \leq 30{,}000$. In Figure 5(a) we show the initial mesh with the periodic interface, as well as two zooms near the interface, while in Figure 5(b), the final mesh is given. As can be seen in the zooms, there are multiple bad cuts that yield large ratios $h_T/\sqrt{h_T^{\min}|\Gamma_T|}$, and consequently, large theoretical efficiency constants C_T on the affected triangles. In addition, the multiplicative factor $(k_{\max}/k_{\min})^{3/2}$ in the efficiency constants C_T and C_F is equal to 10^3. This explains the peak observed at iterations 2 and 3 in Figure 6 for the estimators η, and particularly η_Γ, which also contains the multiplicative factor $\sqrt{h_T}/\sqrt{h_T^{\min}}$. Nevertheless, the estimator is able to cope with these situations and its overall performance is not affected. As seen in Figure 6, we recover the optimal convergence rate $O(N^{-1/2})$ for both the error and the estimator η.

Example 8.3 (Non-smooth interface problem)**.** Finally, we consider a non-smooth interface Γ, which presents a corner. Let $\Omega = [-1,1]^2$ and $\Gamma = \{(x,0);\ x \in [0,1]\} \cup \{(0,y);\ y \in [-1,0]\}$. The interface can be described by

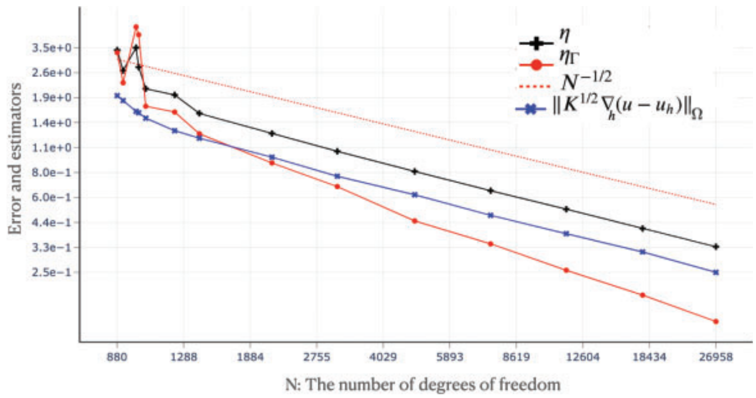

FIGURE 6. Example 8.2. Convergence rate for the error and the estimators η and η_Γ.

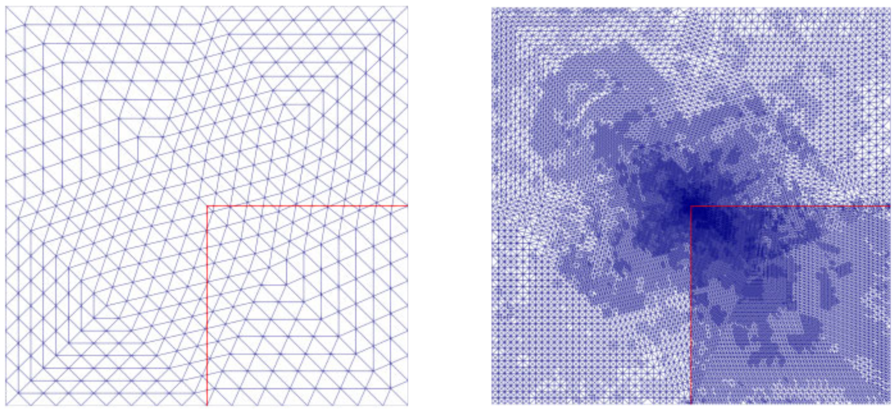

(a) Initial mesh (iteration 0) (b) Final mesh (iteration 10)

FIGURE 7. Example 8.3. Initial and final meshes.

the following level-set function: $\phi(x,y) = y$ if $y > -x$, $\phi(x,y) = -x$ otherwise. The exact solution is given by

$$u(x,y) = \begin{cases} \dfrac{25}{k_1}\, xy(x^2+y^2)^{3/4} & \text{if } \phi(x,y) < 0, \\[2ex] \dfrac{25}{k_2}\, xy(x^2+y^2)^{3/4} & \text{if } \phi(x,y) \geq 0, \end{cases}$$

and satisfies homogeneous transmission conditions and a nonhomogeneous Dirichlet boundary condition.

We set $k_1 = 1$ and $k_2 = 10$. Note that the solution has a singularity at the origin, which coincides with the corner of the interface. The adaptive refinement is performed using the indicator η_T, with the stopping criterion $N \leq 30{,}000$. Figures 7(a) and 7(b) show the initial and final meshes. One can see that the refinement occurs mainly near the origin, as expected. In Figure 8, we observe a behavior similar to that in Figure 6: the estimators η, and particularly η_Γ, exhibit a peak at refinement iteration 2, due to some bad cuts by the interface. Nevertheless, the optimal convergence rate $O(N^{-1/2})$ is recovered.

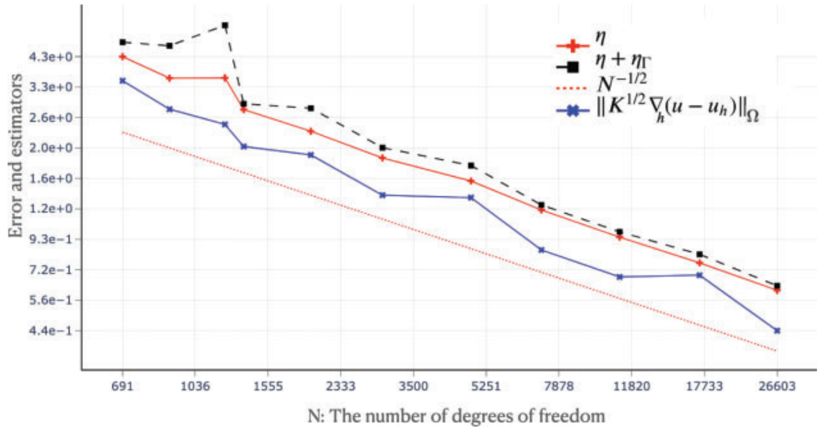

FIGURE 8. Example 8.3. Convergence rate for the error and the estimators η and $\eta+\eta_\Gamma$.

FUNDING

This project has received funding from the European Union's Horizon H2020 Research and Innovation under Marie Curie Grant Agreement No. 945416.

REFERENCES

[1] M. Ainsworth and J.T. Oden, A unified approach to a posteriori error estimation using element residual methods. *Numer. Math.* **65** (1993) 23–50.

[2] M. Ainsworth and J.T. Oden, A posteriori error estimation in finite element analysis. *Comput. Methods Appl. Mech. Eng.* **142** (1997) 1–88.

[3] R. Becker, D. Capatina and R. Luce, Local flux reconstructions for standard finite element methods on triangular meshes. *SIAM J. Numer. Anal.* **54** (2016) 2684–2706.

[4] D. Braess and J. Schöberl, Equilibrated residual error estimator for edge elements. *Math. Comput.* **77** (2008) 651–672.

[5] E. Burman, S. Claus, P. Hansbo, M.G. Larson and A. Massing, Cutfem: discretizing geometry and partial differential equations. *Int. J. Numer. Meth. Eng.* **104** (2015) 472–501.

[6] E. Burman and P. Hansbo, Fictitious domain finite element methods using cut elements: II. a stabilized Nitsche method. *Appl. Numer. Math.* **62** (2012) 328–341.

[7] Z. Cai and S. Zhang, Robust equilibrated residual error estimator for diffusion problems: Conforming elements. *SIAM J. Numer. Anal.* **50** (2012) 151–170.

[8] D. Capatina, A. Gouasmi and C. He, Robust flux reconstruction and a posteriori error analysis for an elliptic problem with discontinuous coefficients. *J. Sci. Comput.* **98** (2024) 8.

[9] D. Capatina, A. Gouasmi and C. He, Elliptic interface problem approximated by CutFEM: I. Conservative flux recovery and numerical validation of adaptive mesh refinement. Preprint arXiv:2507.03492. (2025), submitted.

[10] D. Capatina and C. He, Flux recovery for cut finite element method and its application in a posteriori error estimation. *ESAIM M2AN* **55** (2021) 2759–2784.

[11] P. Destuynder and B. Métivet, Explicit error bounds in a conforming finite element method. *Math Comput.* **68** (1999) 1379–1396.

[12] A. Ern, A.F. Stephansen and M. Vohralìk, Guaranteed and robust discontinuous Galerkin a posteriori error estimates for convection-diffusion-reaction problems. *J. Comput. Appl. Math.* **234** (2010) 114–130.

[13] A. Ern, A.F. Stephansen and P. Zunino, A discontinuous Galerkin method with weighted averages for advection–diffusion equations with locally small and anisotropic diffusivity. *IMA J. Numer. Anal.* **29** (2009) 235–256.

[14] A. Ern and M. Vohralìk, Polynomial-degree-robust a posteriori estimates in a unified setting for conforming, nonconforming, discontinuous Galerkin, and mixed discretizations. *SIAM J. Numer. Anal.* **53** (2015) 1058–1081.

[15] A. Gouasmi, *Numerical flux reconstruction for an interface problem and application to a posteriori error analysis.* Ph.D. thesis, University of Pau and Pays de l'Adour, France (2024).

[16] J. Haifeng, An immersed Raviart–Thomas mixed finite element method for elliptic interface problems on unfitted meshes. *J. Sci. Comput.* **91** (2022) 66.

[17] C. He and X. Zhang, Residual-based a posteriori error estimation for immersed finite element methods. *J. Sci. Comput.* **81** (2019) 2051–2079.

[18] P. Ladevéze and D. Leguillon, Error estimate procedure in the finite element method and applications. *SIAM J. Numer. Anal.* **20** (1983) 485–509.

[19] J.T. Oden, L. Demkowicz, W. Rachowicz and T.A. Westermann, Towards a universal hp adaptive finite element strategy, Part 2. A posteriori error estimation. *Comput. Methods Appl. Mech. Eng.* **77** (1989) 113–180.

[20] P.-A. Raviart and J.-M. Thomas, A mixed finite element method for second order elliptic problems, in *Mathematical Aspects of the Finite Element Method*, Lect. Notes in Math., Vol. 606. Springer-Verlag, Berlin (1977).

[21] R. Verfürth, A posteriori error estimation and adaptive mesh refinement techniques. *J. Comput. Appl. Math.* **50** (1994) 67–83.

[22] R. Verfürth, A note on constant-free a posteriori error estimates. *SIAM J. Numer. Anal.* **47** (2009) 3180–3194.

[23] M. Vohralìk, Guaranteed and fully robust a posteriori error estimates for conforming discretizations of diffusion problems with discontinuous coefficients. *J. Sci. Comput.* **46** (2011) 397–438.